COMPUTATIONAL MODEL OF BREAST CANCER CELL INVASION: EXPLORING THE EGF/CSF-1 PARACRINE SIGNALING BETWEEN MACROPHAGES AND TUMOR CELLS

by

Hildur Knútsdóttir

B.Sc., University of Iceland, 2008

A THESIS SUBMITTED IN PARTIAL FULFILLMENT
OF THE REQUIREMENTS FOR THE DEGREE OF

Master of Science

in the
Department of Physics
Faculty of Science

SIMON FRASER UNIVERSITY
Fall 2012

APPROVAL

Name: Hildur Knútsdóttir

Degree: Master of Science (Physics)

Title of Thesis: Computational model of breast cancer cell invasion: exploring the EGF/CSF-1 paracrine signaling between macrophages and tumor cells

Examining Committee: Dr. J. Steven Dodge, Associate Professor
Chair

Dr. Eirikur Palsson
Senior Supervisor
Assistant Professor, Department of Biology

Dr. Eldon Emberly
Supervisor
Associate Professor

Dr. Jenifer Thewalt
Supervisor
Professor

Dr. Martin Zuckermann
Internal Examiner
Adjunct Professor

Date Approved: November 22, 2012

Partial Copyright Licence

Abstract

Macrophages have been shown, experimentally, to be directly involved in the invasion of breast tumor cells into surrounding tissues and blood vessels. Tumor cells interact with macrophages via a short-ranged signaling pathway involving the epidermal growth factor, EGF, and colony-stimulating factor 1, CSF-1. To study this signaling pathway and the observed motility behaviour of tumor cells I developed a 3D individual cell based computational model. Simulations with my model successfully reproduced results from *in vitro* and *in vivo* experiments. The model can help explain mechanisms responsible for the observed motility behaviour of tumor cells and the noted ratio of 3 invasive tumor cells per 1 invasive macrophage. A parametric sensitivity analysis showed that changing model parameters such as the degradation and secretion of EGF and CSF-1 could alter and even eliminate the invasion of tumor cells. These results yield insight into possible new targets for chemotherapy.

Acknowledgments

I wish to thank, first and foremost, my senior supervisor Dr. Eirikur Palsson for all his support and insightful conversations throughout the course of this study. His guidance during this project has been of utmost importance to me. I would also like to thank my supervisory committee, Dr. Eldon Emberly and Dr. Jenifer Thewalt, for their advice and constructive comments. I would like to extend my gratitude and acknowledge the support and help of Dr. Leah Edelstein-Keshet at the University of British Columbia. Last but not least, I want to thank my family for their invaluable support.

Contents

List of Tables

List of Figures

Chapter 1

Introduction

Every day an average of 62 Canadian women are diagnosed with breast cancer, making it the second most common cancer among Canadian women, trailing only non-melanoma skin cancer [1]. In 2012, an estimate of 5,100 Canadian women will die from breast cancer, comprising 14% of all cancer deaths in women. Hence, it should not come as a surprise that breast cancer is one of the most studied cancers. Some researchers aim to better understand the causes whereas others aspire to find new and improved treatments by understanding how cancer cells behave.

In some types of cancer, including breast cancer, the presence of macrophages at the tumor site relates to poor prognosis. However, in stomach cancer, colorectal cancer and melanoma the presence of macrophages is a positive indicator [2, 3]. Macrophages have many different roles in tumor development and progression. One role is their ability to increase tumor cell motility, which is the focus of this research. Tumor cells and macrophages in close proximity can communicate via a short-ranged chemical signaling loop that results in tumor cells migrating alongside macrophages towards and into blood vessels or surrounding tissues and organs. Once tumor cells get into the blood stream they are difficult to detect and they can extravasate at distant sites in other organs or tissues and form secondary tumors. Secondary tumors, or metastasis as they are also known as, are the primary cause of death in breast cancer patients. Hence, limiting or extinguishing tumor cell motility is a crucial part of cancer treatments. Experiments have shown that when the number of macrophages is decreased at breast cancer sites, tumor progression is slower and fewer cells are able to metastasize, resulting in increased patients survival [4].

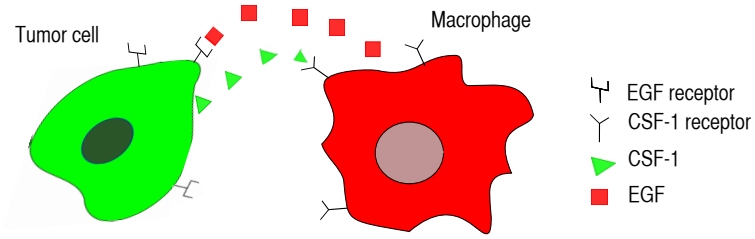

Figure 1.1: Macrophages and tumor cells can interact via a paracrine signaling loop. Tumor cells secrete CSF-1 and have EGF receptors. Macrophages secrete EGF and have CSF-1 receptors. When CSF-1 receptors on macrophages are activated the macrophages respond by secreting EGF and chemotact in the direction of the CSF-1 gradient. When EGF receptors on tumor cells are activated the tumor cells respond by secreting CSF-1 and chemotact along the EGF gradient. This paracrine signaling enables tumor cells to migrate alongside macrophages away from the primary tumor and towards blood vessels or surrounding tissues.

1.1 Biological background

Macrophages are involved in many different stages of tumor development, inflammation, matrix remodelling, angiogenesis, metastasis, intravasation and invasion [2]. They are a type of white blood cell comprising approximately 5% of the body's white blood cell count. Macrophages exist as monocytes in the bloodstream and are recruited to tumor sites by chemotactic factors, one of which is the colony stimulating factor-1, CSF-1 [3]. Over 50% of the cell mass in breast tumors can be constituted of macrophages [5]. The highest concentration of macrophages is at the tumor margin and the concentration decreases with increasing distance from the margin [6]. Macrophages are usually divided into two different categories, perivascular macrophages (PMs), which are located around the blood vessels and play a key role in intravasation and tumor associated macrophages (TAMs) that are distributed throughout the tumor.

Tumor cells manipulate the innate mechanisms of the macrophages via signaling molecules in order to migrate. The tumor cells have epidermal growth factor (EGF) receptors and can secrete CSF-1. The macrophages can secrete EGF and have CSF-1 receptors [7, 8]. Both EGF and CSF-1 receptors are tyrosine kinases receptors [9]. The tumor cells secrete CSF-1, which can bind to the CSF-1 receptors on macrophages and thereby activate them. Activation of CSF-1 receptors starts an internal cascade of events that, among other things, enables the cells to detect a gradient and protrude towards it. Activated macrophages can chemotact in the direction of the CSF-1 gradient

and they will start secreting EGF that can bind to tumor cells. Activated tumor cells respond by secreting more CSF-1 and chemotact in the direction of the EGF gradient. This process results in a short-ranged chemotactic signaling loop that is also called a paracrine loop.

Breast cancer cells migrate alongside macrophages in two different ways, either collective migration, where the two cell types are in direct contact and adhesion is important, or cell streaming, which is observed in the experiments and simulations described here, [10, 11]. The paracrine signaling loop results in macrophages and tumor cells migrating in pairs or in streams where the two cell types alternate. The leader cell can either be a macrophage or a tumor cell, it secretes signaling molecules that attract other cells and it creates tracts by degrading the extracellular matrix. Cell streaming occurs at relatively high speeds in tumors or approximately 4 μm/min.

1.2 Motility of cells

Cancer is a heterogeneous disease and hence, there are multiple different cancer cell lines. Table 1.1 shows the cancer cell lines relevant to this study. The different cell lines have diverse characteristics, some are more aggressive than others and if cancer cells migrate from the primary tumor, treatments become more difficult. The present research focuses on the motility of tumor cells, but not all tumor cells become motile. Research by Philippar *et al.* [11] has shown that motile cells express different mammalian enabled isoforms called Mena isoforms. Mena is a protein that binds actin and is involved in the regulation of cell motility and cell morphology. The invasive and migratory tumor cells have a Mena isoform called Mena^{INV}, whereas the less motile cells express the Mena11a isoform. Cells expressing neither the 11a nor the INV (also called +++) exon are called Mena. Mena cells have increased levels of free barbed end actin filaments at the sites where EGF binds to the cell and the increase in free barbed ends correlates with increased protrusion towards the EGF gradient. Mena^{INV} cells are more sensitive to low gradients of EGF and have a more rapid response to EGF receptor binding. Mena^{INV} cells migrate in a streaming pattern and they are able to detect and migrate towards 25–50 fold lower concentrations of EGF than cells without the Mena isoform. Cells that express Mena11a did not move in a streaming pattern. Such cells have decreased CSF-1 mRNA levels which possibly causes decreased paracrine signaling in addition to making them less sensitive to gradients of EGF. The Mena11a cells have decreased invasion, intravasation and dissemination capabilities. A so called TMEM score (Tumor Micro-Environment for Metastasis) is used in patient treatments as a marker for metastatic risk [12]. TMEM's are regions where tumor cells, containing the Mena^{INV} isoform, macrophages and endothelial cells are located. Patients

with high TMEM scores have a low chance of recovery.

Cell Line	Type	Characteristic	Reference
PyMT	Mouse tumor cell	Known to be highly metastatic (lymph nodes and lungs)	[13]
MTLn3	Rat tumor cell	Highly invasive and metastatic cell line	[14, 15]
MDA-MB-231	Human tumor cell	Largest known number of EGF receptors per cell	[14, 16]
LR5 (RAW264.7)	Mouse macrophage	Rapid immune response, high level of migration response	[17, 18]
BAC (BAC1.2F51.2F5)	Mouse macrophage	Survive and proliferate in presence of CSF-1	[19]

Table 1.1: Cancer cell lines and macrophages used in the experiments relevant for this research.

1.3 Research outline

The objective of this research is to improve the current understanding of the EGF/CSF-1 paracrine signaling loop by simulating the two cell types involved and their reactions to gradients of either EGF (tumor cells) or CSF-1 (macrophages). The simulations should enhance understanding of the mechanisms that contribute to the observed streaming patterns of tumor cells and the noted ratio between invasive tumor cells and macrophages.

Chapter 2 includes a brief overview of some of the key papers that have contributed to our current understanding of the EGF/CSF-1 paracrine signaling loop involved in breast tumor cell motility. These experiments were conducted both *in vitro* and *in vivo* and they highlight the importance of macrophages in tumor cell motility and hence invasion. *In vivo* results indicate that the ratio between collected tumor cells and macrophages seems to always be 3 tumor cells to 1 macrophage. These experiments are the basis of the simulation results in this study. Chapter 3 comprises a detailed description of the computer model which is written in the C programming language. It explains the computational framework used to simulate the two different cell types and the two different signaling molecules and how cells can move in response to chemotactic signals. Chapter 4 presents results from simulations of an *in vitro* experimental setup where the findings regarding the percentage of tumor cells invading collagen are reproduced. I used the model to study how the response of the cells changes with alterations of model parameters related to the cells, such as degradation and secretion coefficients, as well as alterations of external parameters, such as density of macrophages and external chemical concentration. Chapter 5 presents results from *in vivo* experimental setups

where the collection of tumor cells and macrophages into micro-needles containing either EGF or CSF-1, and placed close to a tumor margin, is simulated. I investigated how the observed ratio of 3 collected tumor cells per 1 macrophage can be altered when parameters in the model are changed. Chapter 6 summarizes the results and what has been learned from the simulations. It also includes a list of suggested experiments that will be necessary to validate the model. Chapter 7 includes some future enhancements that can be made to the model once the current results have been validated, as well as suggesting other related biological systems that can be simulated with this computational model. Appendix A contains results from a mathematical analysis of a one dimensional continuum model of the EGF/CSF-1 paracrine loop as well as simulations of the 1D system.

Chapter 2

Experiments

Chemotaxis plays a key role in cell motility in many biological processes such as wound healing, development, inflammation and tumor metastasis [20]. Gradients of various signaling molecules come to play and these chemotaxis systems have been studied in great detail for years both *in vitro* and *in vivo*. Two signaling molecules are of interest in relation to breast cancer cell motility, epidermal growth factor, EGF, and colony-stimulating factor 1, CSF-1. *In vitro* experiments by Goswami *et al.* in 2005 [21] demonstrated that the paracrine signaling loop between macrophages and tumor cells is both necessary and sufficient for tumor cell invasion. In 2004 Wyckoff *et al.* [22] observed *in vivo* that when collection needles containing either EGF or CSF-1 were placed close to a tumor margin in mice both tumor cells and macrophages migrated into the needle and in a somewhat fixed ratio of 3 tumor cells to 1 macrophage. The first direct observation of how this paracrine loop contributes to intravasation was in 2007 by Wyckoff *et al.* [6] using a multiphoton microscope.

2.1 *In vitro* experiments exploring the paracrine loop

The polarization and migration of breast cancer cells towards a gradient of EGF has been verified in experiments. Firstly, in 2005 Soon *et al.* [23] designed a so called Soon chamber to study the motility of MTLn3 breast cancer cells. The chamber is based on a pipette assay to create a 2D EGF gradient. In 2010, Raja *et al.* [24] developed a new device to study chemotaxis of breast cancer cells, called the Nano IntraVital Imaging Device (NANIVID). The experiments using NANIVID were done in 2D and 3D using MTLn3 and MDA-MB-231 cells. The breast cancer cells were explicitly shown to polarize and chemotact up a gradient of EGF.

In vitro experiments by Goswami *et al.* in 2005 [21] were among the first experiments to show

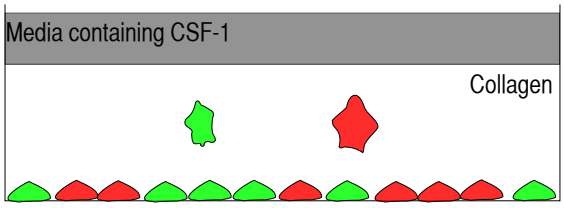

Figure 2.1: The *in vitro* experimental setup from [21]. Tumor cells (labeled with GFP) and macrophages (labeled with Texas red dextran) are plated on a 35-mm MatTek dish, then overlaid by collagen and on top of the collagen there is media containing CSF-1.

that the EGF/CSF-1 paracrine loop between macrophages and tumor cells is both necessary and sufficient for tumor cells to migrate into collagen. The experiments involved plating 50,000 MTLn3 tumor cells labeled with the green fluorescent protein (GFP) on a 35-mm MatTek Dish. In the absence of macrophages the tumor cells were non-polarized. However, when 250,000 macrophages were added to the culture, as well as 36 ng/mL CSF-1, $\sim$25% of the cells had elongated protrusions. In the absence of the external CSF-1 the presence of macrophages only stimulated moderate numbers of protrusions which indicates that the presence of external CSF-1 is necessary to activate the paracrine signaling system. Removing CSF-1 from the mix when no macrophages were present had no effect on the tumor cells, which suggested that CSF-1 is not sufficient for motility but that it is involved in the paracrine loop via macrophages.

Using time lapse microscopy, the motility behaviour of the tumor cells was recorded for 1 hr in the absence and presence of macrophages. Morphometric analysis was used to calculate the directionality of the motility of the cells. When the tumor cells were cultured alone they moved randomly and changed direction frequently. The average speed was measured to be 0.61 μm/min and the net distance moved was 18 μm. When they were cultured with macrophages they moved in a more direct manner towards the macrophages. The average speed was measured to be 0.4 μm/min and the net distance moved was 24 μm. Although the speed of the tumor cells decreases when they are cultured with macrophages, the net distance travelled increases which suggests that the tumor cells do not change direction as much when they are cultured with macrophages.

To study the invasion of tumor cells into collagen, Goswami *et al.* plated 80,000 MTLn3-GFP tumor cells, both in the absence and presence of 200,000 BAC1.2F51.2F5 macrophages, on a 35-mm MatTek Dish. The cells were overlaid by a 750–1,000 μm thick layer of 5–6 mg/ml collagen I. The collagen layer was added to mimic the environment of breast tumor cells. The tumor cells can

move along collagen fibres towards blood vessels where they can intravasate. On top of the collagen was media that contained, among other things, CSF-1 (Figure 2.1). In the absence of macrophages only a few tumor cells migrated into the collagen. However, when the two cell types were plated together $\sim$25% of the tumor cells invaded $>20\mu$m into the collagen. These invasive tumor cells were found in the vicinity of macrophages in the collagen suggesting that the proximity of the two cell types is necessary for invasion. The experiments were repeated with MDA-MB-231 human breast tumor cells and in the presence of macrophages $\sim$70% of the cells invaded $>20\mu$m into the collagen but in the absence of macrophages very few tumor cells became invasive. Both MDA-MB-231 and MTLn3 tumor cells have increased invasion in the presence of macrophages.

In the presence of 12.5 nM EGF, mRNA levels of CSF-1 in tumor cells triple and in the presence of 36 ng/ml CSF-1, mRNA levels of EGF double in macrophages [21]. These results imply that when tumor cells and macrophages are co-cultured in the presence of each other the production of both EGF, in macrophages, or CSF-1, in tumor cells, increases.

Elaborating on these results, Goswami *et al.* [21] explored how blocking either EGF receptors or CSF-1 receptors would affect the invasion of cells. Blocking either of the receptors resulted in a drastic decrease in the number of both cell types invading collagen (50–80% decrease). These results suggest that it is not the macrophages but specifically the EGF molecules that they produce in response to CSF-1 that are necessary for tumor cell invasion and that blocking the paracrine signaling loop decreases the number of invasive cells.

2.2 *In vivo* experiments exploring the paracrine loop

In 2004 Wyckoff *et al.* [22] conducted experiments to study the paracrine loop between tumor cells and macrophages *in vivo* (Figure 2.2). The experiments were conducted with PyMT-induced mammary tumors in mice and a multiphoton microscope to view the process. Tumors were grown for 16 to 18 weeks in the mice after which the mice were anaesthetized and placed under a microscope. Collection needles containing 25 nM EGF were placed approximately 50 μm away from the tumor margin. In 4 hr, approximately 1,000 cells were collected, of which 73% were tumor cells and 26% were macrophages. This ratio of 3:1 between tumor cells and macrophages was also observed when MTLn3 cells were grown in rats. The experiments were repeated, this time with CSF-1 in the collection needle. The results are not shown in Wyckoff *et al.* [22] but they reported that similar results were observed as in the experiments with EGF in the needle.

The experiments with EGF in the needle were repeated for MTLn3 cancer cell line over-expressing

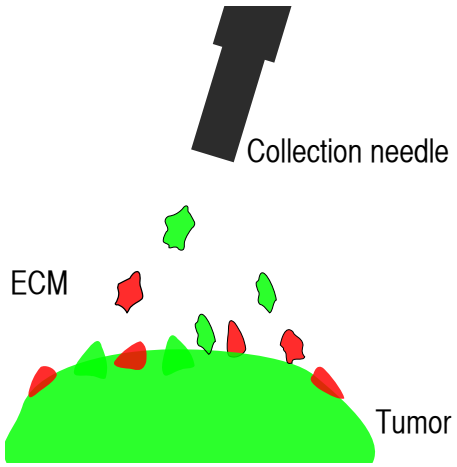

Figure 2.2: The *in vivo* experimental setup from Wyckoff *et al.* [22]. Collection needles containing either EGF or CSF-1 are placed 50 μm away from the tumor margin. Tumor cells and macrophages migrate through the extracellular matrix (ECM) and into the needle.

EGF receptors resulting in a 70–100% increase in collected tumor cells. No mention was made on the number of macrophages collected.

Wychoff *et al.* [22] explored whether the concentration of signaling molecule in the needle would change the number of collected cells. Increasing the concentration of EGF in the needle increased the number of collected cells up to a maximum. Further increasing the amount of EGF in the needle resulted in a decrease in the number of collected cells. With CSF-1 in the needle, increasing the CSF-1 concentration, the number of cells collected increased up to a maximum and then remained unchanged for even higher concentrations of CSF-1 in the needle. Unfortunately, no information about the ratio between collected tumor cells and macrophages for the different concentrations in the needles was noted in the paper.

To gain better understanding of the macrophage role in the migration of tumor cells into collection needles the experiments were repeated with PyMT mice defective in CSF-1 production [22]. These mice are expected to have a low density of macrophages at the tumor sites because CSF-1 concentration is low and thus only few macrophages will be recruited to the tumor site. In these experiments, the number of cells collected in the needles containing either EGF or CSF-1 was significantly decreased (4 to 5 fold) and only 5–7% of the cells were macrophages. The absence of macrophages decreased motility of tumor cells. However, it did not change the growth nor number of tumors.

Wychoff *et al.* [22] also tested the effect of pre-injecting CSF-1 into PyMT tumors (not in the CSF-1 deficient mutant) 4 hr before collection. The addition of external CSF-1 was expected to result in increased number of macrophages at the tumor site because CSF-1 is known to recruit macrophages to tumor sites. A 16% increase was observed in number of cells collected into needles containing 25 nM EGF. The ratio between tumor cells and macrophages remained the same. The experiments were repeated with receptor blockers, for either EGF receptors or CSF-1 receptors, in the needles. Adding the EGF receptor blocker when either EGF or CSF-1 was in the needle resulted in the same number of collected cells as in experiments when neither EGF nor CSF-1 was in the needle. Adding a CSF-1 receptor blocker also resulted in a significant decrease in cells collected, when either EGF or CSF-1 was in the needle, of which $<3\%$ were macrophages. Similar results were noted to be achieved using MTLn3 cells in rats although results were not shown in the paper.

In summary, Wychoff *et al.* [22] showed that the paracrine loop between tumor cells and macrophages is necessary for tumor cell invasion in mice for the cell lines that they tested. Either EGF or CSF-1 in the collection needles could initiate the paracrine signaling loop and experiments with 25 nM EGF in the needles resulted in a ratio of 3 invasive tumor cells per 1 invasive macrophage. Decreasing the density of tumor cells at the tumor sites resulted in a significant decrease in the number of collected cells. Blocking either EGF or CSF-1 receptors resulted in a significant decrease in number of cells collected in the needles.

The EGF/CSF-1 paracrine signaling loop has been studied by other researchers who also concluded that paracrine signaling is necessary for breast cancer cell motility. Lin *et al.* [4] conducted *in vivo* experiments in PyMT mice with null mutation in the CSF-1 gene. Compared to the wild type, the CSF-1 mutant did not show altered number of tumors or growth, but did however alter the tumor cell invasiveness and metastatic potential as well as the number of macrophages at the tumor site. Experiments with up-regulated CSF-1 production accelerated the invasiveness and the promotion of macrophages to the tumor site. Experiments where CSF-1 was down-regulated slowed down tumor progression and metastasis but did not alter the tumor development. Kirma *et al.* [25] conducted similar experiments but explored both CSF-1 and CSF-1 receptor up-regulation and focused on their effect on carcinogenesis. Increased expression of CSF-1 and CSF-1 receptors result in changes before the formation of the primary tumor that could lead to tumor growth at later stages in development.

2.3 *In vivo* experiments to study intravasation

In 2007, Wyckoff *et al.* [6] were the first to directly observe the role of macrophages in intravasation using a multiphoton microscope. The experiments were done using mouse models with the PyMT cell line. Tumor cells were labeled using GFP and macrophages were labeled using Texas red-dextran. Macrophages usually exist in high concentration at the tumor margin but the concentration decreases within the tumor. Over 80% of tumor cell motility was observed to be associated with macrophages both at the tumor margin and deep within a tumor in association with perivascular macrophages, PMs. More tumor cells move at the tumor margin where more macrophages are located. When the motility was normalized to the number of macrophages, tumor cells in the vicinity of PMs moved more frequently and they migrated towards the blood vessels. This suggests that tumor associated macrophages (TAMs) and PMs behave differently, PMs seem to have an amplified effect on tumor cell motility. The average speed of tumor cells moving with PMs was 3.9 ± 0.28 μm/min (calculated from 20 different cells in 8 different mice). Motility of tumor cells at the tumor margin is believed to be responsible for tumor cell invasion into surrounding tissues whereas tumor cell motility associated with PMs is responsible for intravasation and metastasis.

2.4 Experiments with different MENA isoforms

As mentioned in the previous chapter, invasive tumor cells express a different Mena isoform than non-invasive cells. Philippar *et al.* [11] studied the different effects of Mena (not containing a specific exon), Mena11a and Mena^{INV}. Mena11a is expressed in poorly invasive benign tumors but Mena^{INV} is expressed in invasive and metastatic tumors. In the experiments, intravital imaging (IVI) and MTLn3 cells in mice were used. Mena was observed to be localized at cell-cell junctions and at sites of rapid protrusion. Cell protrusion is the first step in cell motility and therefore it was studied in greater detail. In motile cells, Mena and Mena^{INV} was distributed throughout the cytoplasm and existed in greater concentration at the leading edge. The presence of Mena^{INV} corresponded to increased number of motile cells. Mena expressing cells had a moderate increase in lung metastasis compared to the control cells. However, Mena^{INV} cells had a dramatic increase in lung metastasis.

Elaborating on these results Philippar *et al.* [11] explored whether Mena and Mena^{INV} affected invasion *in vitro*. The experiment by Goswami *et al.* [21], described in chapter 2.1, was repeated but now with cells expressing either Mena or Mena^{INV}. In the presence of macrophages, both cell

types had similar amount of invasive cells as the parental MTLn3 cells and therefore they concluded that the invasion potential was at its maximum in parental MTLn3 cells. Increasing the sensitivity of tumor cells to a gradient of EGF did not increase the invasiveness of the tumor cells. In the absence of macrophages, Mena expressing cells showed increased invasion and Mena^{INV} cells showed an even greater increase in invasion. Philippar *et al.* hypothesized that moderate amounts of EGF receptor ligands in the media overlaying the collagen were diffusing down and causing increased invasion. The hypothesis was tested by using EGF receptor inhibitors which resulted in the invasion decreasing to the same level as the control cells. These results indicate that Mena and Mena^{INV} cells are more sensitive to lower concentrations of EGF than the parental MTLn3 cells. In the experiments with MTLn3 cells, the concentration of EGF ligands in the media above the collagen was below a threshold level for detection. The Mena and Mena^{INV} cells have a lower threshold value for detection and therefore when the experiments were repeated with these cells they were observed to invade the collagen.

Philippar *et al.* [11] investigated the EGF sensitivity of Mena^{INV} cells by exploring the invasion response due to different chemical gradients. *In vitro* Mena^{INV} cells could respond to EGF levels as low as 0.025 nM whereas the control cells had a threshold EGF level around 1 nM. The maximum response level of Mena^{INV} cells was 5 nM and the invasion response decreased at higher EGF levels. *In vivo* a similar biphasic response occurs, but the maximum increased to 25 nM. In addition to increased sensitivity Mena^{INV} cells also had a faster response, they started protruding within 10 s whereas Mena and control cells required 30–90 s. I explored this in my simulations by using different concentrations of EGF in collection needles placed close to a tumor margin.

In order for cells to migrate, they need to be able to dissociate from a primary tumor and cross a basement membrane. *In vitro* this occurs at invadopodia by local activation of proteases. Philippar *et al.* [11] hypothesized that 3D protrusions correlate to invadopodia *in vitro* and tested the effect of Mena and Mena^{INV} on invadopodia. The number of invadopodia of Mena and Mena^{INV} were similar to that of the control cells. However, there was a significant increase in matrix degradation of cells expressing Mena and Mena^{INV}. The researchers found that in these cell types the invadopodium had longer lifetimes and examining the actin structure showed that the invadopodium in Mena and Mena^{INV} cells were more stable.

In conclusion, Mena and Mena^{INV} cells are more motile and invade surrounding tissues and intravasate blood vessels. Mena11a cells on the other hand are not invasive but found in primary tumors. Mena and Mena^{INV} cells are more sensitive to EGF gradients and increase matrix degradation by stabilizing invadopodia. Mena^{INV} cells are more sensitive to gradients of EGF than Mena

cells and they start protruding earlier. I tested the invasive potential of cancer cells with different Mena isoforms by changing the EGF threshold concentration for a tumor cell response and by changing the amount of chemical degraded by tumor cells in the simulations and comparing these results.

Chapter 3

Computational framework

To better understand the EGF/CSF-1 paracrine loop between tumor cells and macrophages I further developed a 3D discrete computational model first designed by Palsson [26] over a decade a go. Palsson [26] used the model to study cyclic AMP signaling and cell motility in Dictyostelium discoideum (Dd). I modified the computational framework to simulate the motility of cancer cells and to include the paracrine signaling loop. In my model, there are two different cell types, macrophages and tumor cells, which are represented as individual deformable ellipsoids. There are also two different signaling molecules, EGF and CSF-1, the concentration of which is approximated using a set of partial differential equations. The model is written in the C programming language and it produces 3D images using the graphic program openGL.

3.1 Cells

Both macrophages and tumor cells can form multiple protrusions which results in them having asymmetric shapes. In this model, the two cell types are approximated as individual deformable ellipsoids with constant volume, V. Each axis of the ellipsoid has a Hookean spring, κ_2, in parallel with a Maxwell element, which consists of a viscous element, μ, in series with a Hookean spring, κ_1 (Figure 3.1). The Maxwell element controls the relaxation of the axis once a force acting on it is removed. This model, comprising of two Hookean springs and a viscous element for each axis, has often been used to represent the viscoelastic properties of cells. κ_1 represents the initial elastic response of a cell to deformation, μ represents the steady deformation of a cell under constant force and κ_2 prevents the cells from being squished or stretched too much on any given axis. The three axes of the ellipsoids are represented with the vectors $\vec{a}$, $\vec{b}$ and $\vec{c}$. When one axis is stretched

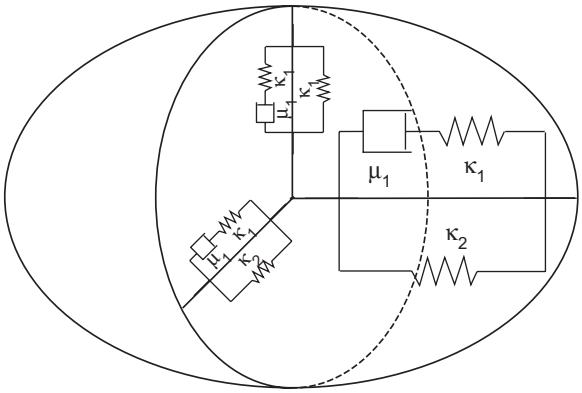

Figure 3.1: Cells are represented as deformable ellipsoids where each axis is represented by a Hookean spring with spring constant κ_1 in parallel with a Maxwell element consisting of viscous element μ and a Hookean spring κ_2. Figure from Palsson [26].

another one needs to be compressed in order to preserve the volume of the ellipsoid. This generates a modifying force, F_{mod}, which can be calculated by solving equations 3.1 and 3.2 simultaneously.

$$\frac{dr_i}{dt} = \frac{\kappa_1(F_i - F_{mod})}{\mu(\kappa_1 + \kappa_2)} + \frac{dF_i/dt}{(\kappa_1 + \kappa_2)} - r_i\frac{\kappa_1\kappa_2}{\mu(\kappa_1 + \kappa_2)} \tag{3.1}$$

$$r_a r_b r_c = (r_a + \Delta r_a)(r_b + \Delta r_b)(r_c + \Delta r_c) = V/(\frac{4}{3}\pi) \tag{3.2}$$

where r_i are the lengths of the different axes of the ellipsoid, i can be a, b or c, F_i is the total force acting on axis i and Δr_i is the change in length of axis i. When the force is removed the ellipsoid slowly relaxes back to its original shape.

Before the cell begins to move it polarizes and establishes a front and back. In the model, to account for this the a axis of the ellipsoidal cells is always oriented in the direction the cell is moving in. If the concentration of a signaling molecule, either EGF or CSF-1, around a cell is above a set threshold and the signaling molecule gradient is steep enough, the cell will orient its a axis in the direction of the gradient and start moving along it. The gradient calculated is the absolute gradient across the cell diameter. If the gradient is below a set threshold the cells will chose a random direction with a biased towards the previous direction. When the unit-vector $\vec{\mathbf{a}}$ of the ellipsoid is rotated in the new direction that the cell is moving in, the new $\vec{\mathbf{b}}$ and $\vec{\mathbf{c}}$ unit-vectors also need to be calculated. The new unit-vectors are calculated using the Gram Schmidt process for an orthogonal

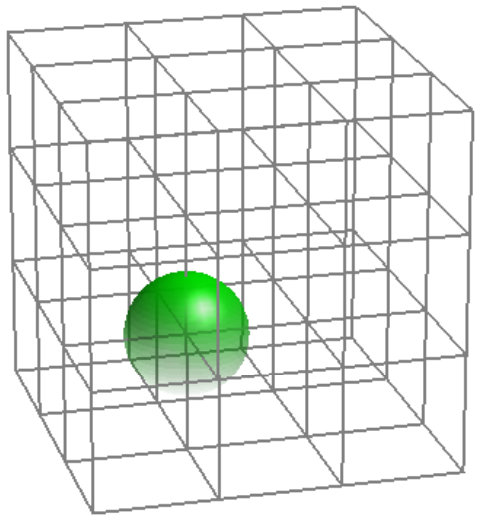

Figure 3.2: Demonstration of how a cell (green sphere) can move independently of the lattice cubes used to calculate chemical concentrations. Here, the green cell has volume in 8 different lattice cubes, which needs to be accounted for when calculating chemical concentration and secretion.

basis where the old $\vec{\mathbf{b}}$ and $\vec{\mathbf{c}}$ vectors are used as the previous orthonormal basis. The lengths of the new $\vec{\mathbf{a}}$, $\vec{\mathbf{b}}$, and $\vec{\mathbf{c}}$ vectors (r_a, r_b and r_c) are calculated by finding where the new vectors would cut the surface of the old ellipsoid. The force acting on a cell, further explained in section 3.4, determines how much the ellipsoidal cells deform. The deformability of the ellipsoids helps visualize the cells polarity and in practice represent the protrusion of cells along a chemical gradient. Using semi-hard spherical cells in my simulations would have produced quantitatively similar results. However, since I hope to extend this work to simulate intravasation and extravasation of tumor cells, using ellipsoidal cells becomes important and does not add much to the computational time. For these simulations, the cells will need to squeeze through the walls of the blood vessels and the deformability of cells will be necessary.

3.2 Concentration of signaling molecules

The tumor cells involved in the paracrine signaling loop with macrophages, secrete CSF-1 in response to a local EGF concentration above a set threshold. Similarly, macrophages secrete EGF in response to a high enough local CSF-1 concentration. The concentration of the two signaling

molecules is calculated on a 3D grid where each side in a lattice cube is one cell diameter in length. Every time step, the concentration in all lattice cubes is used to find the local chemical concentration around each cell and to calculate the chemical gradients. Cells are free to move around independently of this grid and therefore each cell can partially occupy up to 8 different lattice cubes at a given point in time (Figure 3.2). This partial overlap is accounted for when calculating the local concentration around a cell. The overlap is also used to determine how the cell's secretion is distributed to the overlapping grid cubes. The local concentrations around the cells is calculated using the following equations:

$$[C]_{cell-q} = \sum_{i=l-1}^{i=l+1} \sum_{j=m-1}^{j=m+1} \sum_{k=n-1}^{k=n+1} \frac{S_{cell-q}^{ijk}}{S_{cell}} [C]^{ijk} \tag{3.3}$$

$$[E]_{cell-p} = \sum_{i=l-1}^{i=l+1} \sum_{j=m-1}^{j=m+1} \sum_{k=n-1}^{k=n+1} \frac{S_{cell-p}^{ijk}}{S_{cell}} [E]^{ijk} \tag{3.4}$$

where $[C]_{cell-q}$ is the CSF-1 concentration around macrophage q, the centre of macrophage q is located in a lattice cube with (x,y,z)-coordinates lmn, $[C]^{ijk}$ is the CSF-1 concentration in lattice cube ijk, S_{cell} is the total surface area of a cell, S_{cell-q}^{ijk} is the segment of surface area of macrophage q that is located in lattice cube ijk, $[E]_{cell-p}$ is the EGF concentration around tumor cell p, S_{cell-p}^{ijk} is the segment of surface area of tumor cell p that is located in lattice cube ijk and $[E]^{ijk}$ is the EGF concentration in lattice cube ijk. The local concentration around a cell needs to be above a certain threshold ($[E]_{th}$ for tumor cells or $[C]_{th}$ for macrophages) for the cell to begin secreting a signaling molecule. The secretion of CSF-1 by tumor cells and EGF by macrophages can be approximated using Michaelis Menten kinetics:

$$\Omega'([E]_{cell-p}) = \frac{[E]_{cell-p}^n}{[E]_{th}^n + [E]_{cell-p}^n} \tag{3.5}$$

$$\Omega'([C]_{cell-q}) = \frac{[C]_{cell-q}^n}{[C]_{th}^n + [C]_{cell-q}^n} \tag{3.6}$$

where $\Omega'([E]_{cell-p})$ is the secretion of CSF-1 by tumor cell p in response to its local EGF concentration. Similarly, $\Omega'([C]_{cell-q})$ is the secretion of EGF by macrophage q in response to its local CSF-1 concentration and $n \geq 1$. For large n this equation has a sharp transition threshold (Figure 3.3). Presuming that there is a sharp transition when these cells start secreting signaling molecules, equations 3.5 and 3.6 can be approximated with the following equations for simplicity:

$$\Omega([E]_{cell-p}) = \begin{cases} 0 & \text{if } [E]_{th} > [E]_{cell-p} \\ \frac{[E]_{cell-p}}{1+[E]_{cell-p}} & \text{if } [E]_{th} \leq [E]_{cell-p} \end{cases} \tag{3.7}$$

$$\Omega([C]_{cell-q}) = \begin{cases} 0 & \text{if } [C]_{th} > [C]_{cell-q} \\ \frac{[C]_{cell-q}}{1+[C]_{cell-q}} & \text{if } [C]_{th} \leq [C]_{cell-q} \end{cases} \tag{3.8}$$

Below a set threshold in the model ($[E]_{th}$ and $[C]_{th}$) there is no chemical secretion by the cells. Using a sigmoidal term instead of the transition threshold assumed here, does not affect the results qualitatively. The secretion of either EGF or CSF-1 from each cell must be distributed into all the lattice cubes that the cell is located in, therefore the secretion in each lattice cube becomes:

$$C_{sec}^{ijk} = \sum_{p \in (ijk)} \frac{S_{cell-p}^{ijk}}{S_{cell}} k_{sec-p}^{tumor} \mathcal{H}([E]_{cell-p} - [E]_{th}) \frac{[E]_{cell-p}}{1 + [E]_{cell-p}} \tag{3.9}$$

$$E_{sec}^{ijk} = \sum_{q \in (ijk)} \frac{S_{cell-q}^{ijk}}{S_{cell}} k_{sec-q}^{macro} \mathcal{H}([C]_{cell-q} - [C]_{th}) \frac{[C]_{cell-q}}{1 + [C]_{cell-q}} \tag{3.10}$$

where C_{sec}^{ijk} is the total amount of CSF-1 secreted by all tumor cells located in lattice cube ijk in each time step, the sum is over all tumor cells p that have some surface area (S_{cell-p}^{ijk}) in lattice cube ijk, k_{sec-p}^{tumor} is the CSF-1 secretion coefficient for tumor cell p, $\mathcal{H}$ is the Heaviside function. Similarly, E_{sec}^{ijk} is the total amount of EGF secreted by all macrophages located in lattice cube ijk in each time step, the sum is over all macrophages q that have some surface area (S_{cell-q}^{ijk}) in lattice cube ijk and k_{sec-q}^{macro} is the EGF secretion coefficient for macrophage q.

In each time step in the simulations, the change in concentration of the signaling molecules needs to be calculated with respect to the diffusion of the molecules, the secretion of signaling molecules by cells and the degradation of signaling molecules at cell membrane and in the extracellular matrix. This is done using the following reaction-diffusion partial differential equations:

$$\begin{aligned} \frac{d[C]^{ijk}}{dt} &= \mathcal{D}\nabla^2[C]^{ijk} + C_{sec}^{ijk} - k_{deg}^{csf^{ijk}}[C]^{ijk} \\ \frac{d[E]^{ijk}}{dt} &= \mathcal{D}\nabla^2[E]^{ijk} + E_{sec}^{ijk} - k_{deg}^{egf^{ijk}}[E]^{ijk} \end{aligned} \tag{3.11}$$

where $\mathcal{D}$ is the diffusion coefficient for EGF and CSF-1 and $k_{deg}^{csf^{ijk}}$ and $k_{deg}^{egf^{ijk}}$ are the degradation coefficients for CSF-1 and EGF, respectively (further explained in section 3.3). The partial differential equations 3.11 are solved in each lattice cube in every time step using forward Euler's method with no flux boundary conditions.

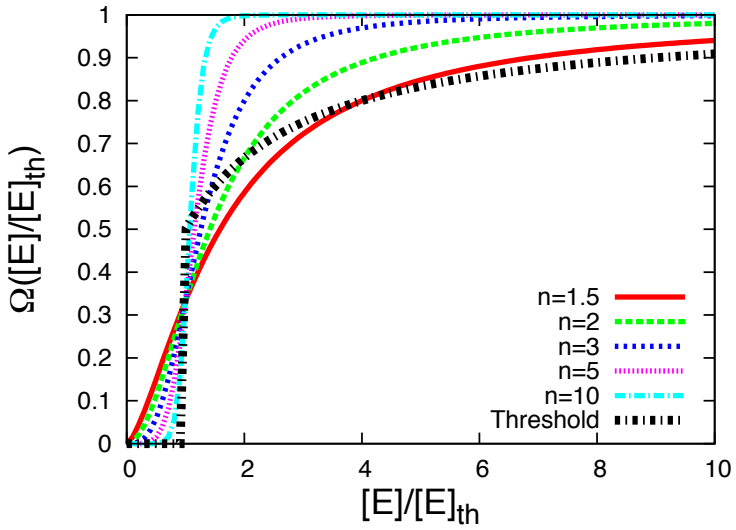

Figure 3.3: Plot of equations 3.5 and 3.7. For n=1.5, 2, 3, 5, 10. The black line is the approximation used in the model for the Michaelis Menten kinetics.

In order for a tumor cell (macrophage) to start secreting CSF-1 (EGF) the local chemical concentration of EGF (CSF-1) has to be above a set threshold. However, in order for a cell to start migrating in the direction of the gradient both local concentration and steepness of gradient need to be above a set threshold in the model.

3.3 External and membrane-bound degradation

There are two different means of degradation in the model, membrane-bound degradation, k_{mem}, and external degradation, k_{ext}. Thus, the degradation coefficients in each lattice cube, ijk, are determined with the following equations:

$$\begin{aligned} k_{deg}^{csf^{ijk}} &= k_{ext}^{ijk} + \left(\sum_{p \in (ijk)} \frac{S_{cell-p}^{ijk}}{S_{cell}} + \sum_{q \in (ijk)} \frac{S_{cell-q}^{ijk}}{S_{cell}} \right) k_{mem}^{csf} \\ k_{deg}^{egf^{ijk}} &= k_{ext}^{ijk} + \left(\sum_{p \in (ijk)} \frac{S_{cell-p}^{ijk}}{S_{cell}} + \sum_{q \in (ijk)} \frac{S_{cell-q}^{ijk}}{S_{cell}} \right) k_{mem}^{egf} \end{aligned} \tag{3.12}$$

where k_{mem}^{csf} is the membrane-bound degradation coefficient of CSF-1 for each cell and k_{mem}^{egf} is the

membrane-bound degradation coefficient of EGF for each cell. Equation 3.12 enables each cell type to break down either EGF or CSF-1 or both. The external degradation coefficient, k_{ext}^{ijk}, is assumed to be uniform and the same for both EGF and CSF-1.

Membrane-bound degradation is caused by enzymes on the cell membrane. External degradation occurs in the extracellular matrix and can be due to enzymes from the cell membranes that have been cleaved off and are now free to diffuse through the extracellular matrix. The external degradation constant is also used to account for perfusion. Perfusion is the continuous addition and removal of material in the extracellular matrix caused by fluid flow. Assuming perfusion is constant we can model it as external degradation.

3.4 Forces

In order to determine the movement of each cell, all the active and repulsive forces acting on the cell are calculated using the following equation:

$$\mathbf{F}_{cell} = \mathbf{F}_{active} + \sum_{N} \mathbf{F}_{repulsive} \tag{3.13}$$

where N is the number of neighbouring cells that exert a repulsive force on the cell. Cells grab onto the extracellular matrix (i.e. collagen fibres) to generate an active force, $\mathbf{F}_{active}$, that moves them either in the direction of a gradient or in a random direction.

$$\mathbf{F}_{active} = \begin{cases} \mathbf{F}_{random} & \text{if } \nabla[A]_{th} > \nabla[A], \text{ where } A \in \{E, C\} \\ \mathbf{F}_{chemotax} & \text{if } \nabla[A]_{th} \leq \nabla[A], \text{ where } A \in \{E, C\} \end{cases} \tag{3.14}$$

where $\mathbf{F}_{random}$ represents the random and exploratory behaviour of a cell, $\mathbf{F}_{chemotax}$ represents the force generated for a cell to chemotact in the direction of a gradient and $\nabla[A]$ is the gradient of either EGF if the cell is a tumor cell or CSF-1 if the cell is a macrophage and $\nabla[A]_{th}$ is the threshold value in the model above which the gradient needs to be for the cell to chemotact along that gradient. The a axis of the cell is always oriented in the direction that the cell is attempting to move, be it in the direction of the chemical gradient or in a random direction. Therefore, the direction of the active force is given as $\vec{\mathbf{F}} = F\vec{\mathbf{a}}$, where $\vec{\mathbf{a}}$ is the unit vector for the a axis. The magnitudes of the two active forces are given in Table 3.1.

There is a repulsive force between cells in close proximity to ensure they do not overlap, it is calculated from the following equation:

$$\mathbf{F}_{repulsive} = \begin{cases} 0 & \text{if } x > 0 \\ F_{compress}(-x)^{\frac{9}{5}} \cdot \frac{\vec{\mathbf{r}}_{ij}}{\|\vec{\mathbf{r}}_{ij}\|} & \text{if } x \leq 0 \end{cases} \tag{3.15}$$

where $F_{compress}$ is the strength of the repulsive force, $x = \frac{d}{r_{cell}}$, where d is the distance between the surface of the two cells along the vector $\vec{r}_{ij}$ between the centre of the two cells and r_{cell} is the radius of the cells (5 μm).

Each time step all forces acting on every cell are calculated and then all the cells are moved at the same time. The cells are moving in a very low Reynolds number environment, so I can ignore inertia. Therefore, the active and repulsive forces are balanced by the drag force, resulting in the following equation of motion:

$$\frac{d\mathbf{x}_i}{dt} = \mathbf{v}_i \tag{3.16}$$

$$\mathbf{v}_i = \frac{\mathbf{F}_{cell}}{\mu_{ecm}} \tag{3.17}$$

where $d\mathbf{x}_i$ is the change in position of cell i for a time step Δt = 0.01 min, $\mathbf{v}_i$ is the velocity of cell i and μ_{ecm} is the viscosity between the cells and the extracellular matrix. μ_{ecm} is estimated from experimental data of cell velocity and the force the cells apply to their surroundings. The shape of the cells does not change significantly and thus μ_{ecm} is assumed to be constant.

3.5 Parameters

In Table 3.1 I list the parameters that are used in the model. These parameters are kept fixed in all my simulations. Some of the parameters are found in the literature and I have listed the reference for those in the table, others are estimated to fit observations from experiments. In the simulations, model parameters that are not listed in Table 3.1, such as degradation and secretion coefficients for the signaling molecules as well as the initial external chemical concentration and number of cells, are altered to investigate the effect they have on the motility of the macrophages and tumor cells. Those parameters are listed in later chapters.

3.6 Outline of simulations

Below is the outline and order of the actions that are performed each time step in the simulations. The time step is 0.01 min and each grid cube is 10 μm in length.

Parameter	Value	Reference
D	4×10^{-4} mm^{2}min^{-1}	[27]
r_{cell}	5 μm	[6]
$[E]_{th}$	0.1 nM	[11]
$[C]_{th}$	0.1 nM	[11]
k_1	4×10^{2} nN/μm	
k_2	2 nN/μm	
μ	6×10^{-6} dyne·s/μm	
μ_{ecm}	8×10^{-3} dyne·s/μm	
$F_{chemotax}$	0.2 nN	
F_{random}	0.1 nN	
$F_{compress}$	30 nN	

Table 3.1: **Parameters** - List of parameters used in the model. When parameter values could be found in the literature they were used in the model (see **Reference** column). Often, parameter values could not be obtained from the literature in which case the model parameters were fitted to match observations from experiments. Other parameters, such as the degradation and secretion coefficients, are altered in the simulations and those parameters are listed in later chapters.

1. Cells are randomly distributed at a given initial density and cell ratio that depends on the simulation.

2. The local concentration of signaling molecules (EGF and CSF-1) for each cell is calculated (equations 3.3 and 3.4) and the EGF and CSF-1 secretion from every cell determined. The cell secretion is then divided into the lattice cubes according to equations 3.9 and 3.10 and the diffusion and degradation of EGF and CSF-1 is calculated using equations 3.11.

3. If a cell detects a gradient above a set threshold, the a axis of the cell is oriented along the gradient. Otherwise, the cell orients in a random direction biased towards the direction it was moving in.

4. All the active and repulsive forces acting on each cell are calculated.

5. The cells are then moved using the equation of motion (equation 3.16). Start again at step 2.

3.7 Continuum model

I have also investigated the EGF/CSF-1 paracrine signaling pathway with a one-dimensional continuum model to explore the parameter space and identify conditions necessary for instability, see

appendix A. I used a set of four partial differential equations to describe the system and assumed a linear relation for the secretion of signaling molecules with respect to density of cells, while ignoring the membrane-bound degradation. The limitations of the parameter space as identified by the linear stability analysis of the 1D system were also observed in simulations with the 3D model.

Chapter 4

Results from simulations of *in vitro* experiments

In the experiments, described in chapter 2.2, Goswami *et al.* [21] plated 80,000 tumor cells and 200,000 macrophages on a MatTek dish. That corresponds to a ratio of about 30% tumor cells and 70% macrophages. Approximately 25% of the MTLn3 tumor cells were found to invade more than 20 μm into collagen placed above them and these invasive tumor cells were in close proximity to macrophages.

The simulations in this chapter were designed to emulate the *in vitro* experimental setup from Goswami *et al.* [21]. The ratio between the two cell types was the same as in the experiments but with a total of 100 cells. Simulation results using more cells, total cell numbers ranging from 100–2500 and the same macrophage to tumor cell ratio and density, were qualitatively comparable in regards to percentage of invasive cells. In light of this, I ran the simulations in this chapter with 100 cells to reduce simulation time.

To explain the motility behaviour of the tumor cells and macrophages in the simulations, I will define a few of the observed phenomena:

- **Invasive cells**: Cells that invade more than 20 μm into the collagen matrix, in the simulations this corresponds to moving more than 20 μm in the positive z-direction.
- **Sub-threshold gradient**: When the gradient of EGF (CSF-1) is below the threshold value for detection for a tumor cell (macrophage). The sub-threshold gradient results in cells not chemotacting along a gradient.

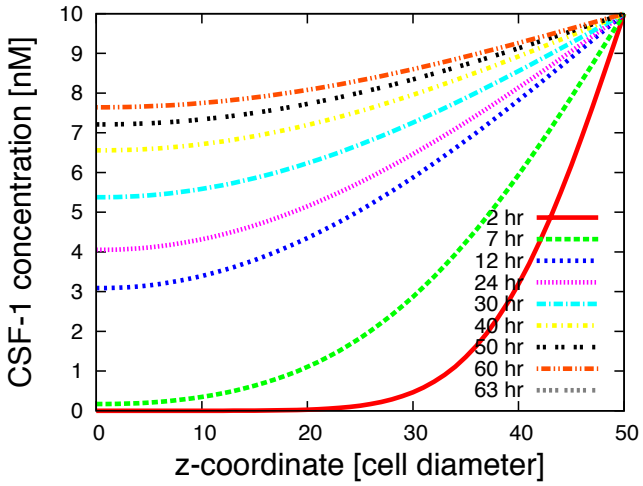

Figure 4.1: Average external CSF-1 concentration as a function of height from bottom of plate (z coordinate) at different times in simulation. Concentration of CSF-1 at the top was kept fixed and the concentration at the plate increased with time. There were no cells present in this simulation.

- **Sub-threshold concentration**: When the signaling molecule concentration around a cell is below the concentration threshold value in the model. Sub-threshold concentration results in cells not chemotacting along a gradient and not secreting any signaling molecules.

- **Chemotaxis failure:** When the cells can not chemotact along a gradient from the overlaid media or from other cells because the concentration of signaling molecules at the plate or tumor margin has an attenuating effect on the gradient.

In the experiments, the overlaid media contained CSF-1 (Figure 2.1). This is approximated in the simulations by placing a uniform concentration of CSF-1 500 μm above the cells. Presuming a large media volume with high CSF-1 concentration the overlaid media in the simulations was assumed to have a constant CSF-1 concentration. Figure 4.1 shows the results from a simulation where there is no degradation nor secretion so the CSF-1 concentration in the collagen continues to increase. If the simulation is kept running for long enough the whole area would have a uniform concentration.

Simulations without degradation, neither membrane-bound nor external, resulted in two distinctly different results depending on the value of the CSF-1 secretion coefficient, k_{sec}^{tumor}, for tumor cells. (a) When k_{sec}^{tumor} = 0.03 nM/min there were no invasive cells and (b) when k_{sec}^{tumor} =

0.003nM/min all the cells became invasive (Figure 4.2). In (a) the CSF-1 secreted by the tumor cells builds up too fast at the bottom of the plate. This interferes with the CSF-1 concentration profile so that the gradient is no longer towards the CSF-1 in the overlaid media and thus the macrophages do not invade. This is an example of chemotaxis failure. If no macrophages are invasive the tumor cells can not invade either because they migrate along an EGF gradient from macrophages. In (b) the gradient towards the top persists and all of the cells become invasive. The tumor cells follow far behind the macrophages in these simulations, which does not match experimental results. I therefore concluded that, degradation is necessary to simulate the EGF/CSF-1 paracrine signaling loop involved in invasion of breast tumor cells.

Simulations also showed that with low external degradation and no membrane-bound degradation there were no invasive cells. For high external degradation and no membrane-bound degradation there were only invasive macrophages. These results suggest that membrane-bound degradation is necessary to explain the experimental results.

In this chapter, I will explore how changing parameters such as degradation coefficients, secretion coefficients, external concentration of CSF-1 and initial ratio between tumor cells and macrophages affects the percentage of invasive cells. I will also investigate two different scenarios of membrane-bound degradation. In the first scenario the tumor cells only degrade EGF and the macrophages degrade CSF-1. In the second scenario both cell types degrade EGF and CSF-1.

In the figures of the simulations, red cells are macrophages and green cells are tumor cells. The two bars on the right represent the chemical concentration in the centre of the x-y plane at different heights, the red bar represents CSF-1 and the green bar represents EGF (Figure 4.3). All graphs that show the change in percentage of invasive cells for different parameters are average values for 10 differently randomized simulations.

4.1 Generating the desired percentage of invasive tumor cells

The percentage of invasive cells in the simulations depends on the choice of parameters. Changing the parameter values can alter the percentage of invasive cells. Goswami *et al.* [21] observed in their experiments that approximately 25% of the MTLn3 tumor cells were invasive. To obtain a similar percentage in the simulations I used the following set of parameters and initial conditions: The activated macrophages secrete two thirds more EGF than the activated tumor cells secrete CSF-1. These values are based on results from mRNA experiments in Goswami *et al.* [21]; The CSF-1 membrane-bound degradation is four times higher than the EGF membrane-bound degradation;

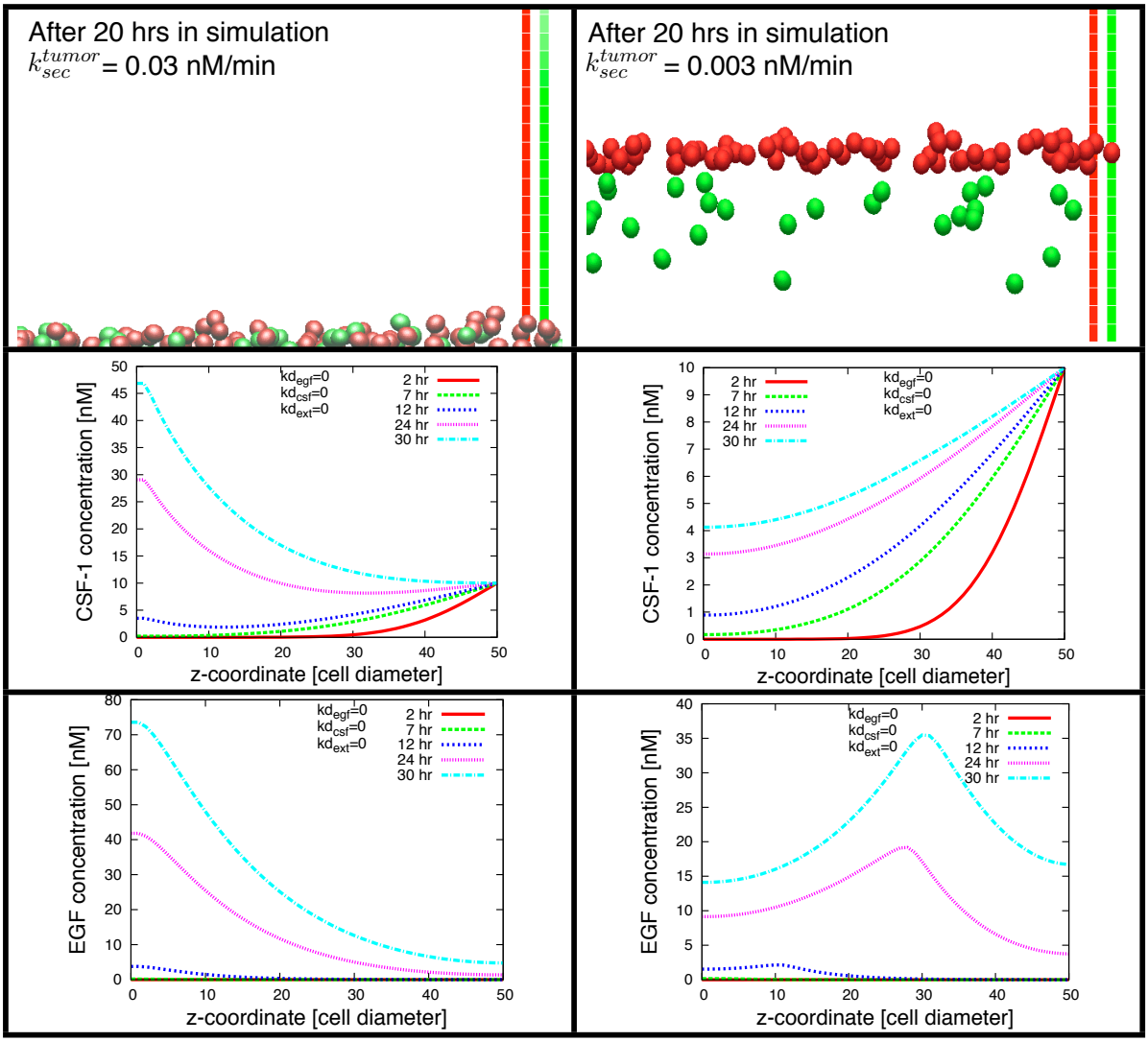

Figure 4.2: Snapshots from simulations after 20 hours when there was no degradation. In the left column k_{sec}^{tumor} = 0.03nM/min and in the right column k_{sec}^{tumor} = 0.003nM/min. Red cells are macrophages and green cells are tumor cells. The red bar on the right represents the average concentration of CSF-1 and the green bar on the right represents the average concentration of EGF. The second row shows the average concentration of CSF-1 at different times in simulation. The third row shows the average EGF concentration at different times in simulation.

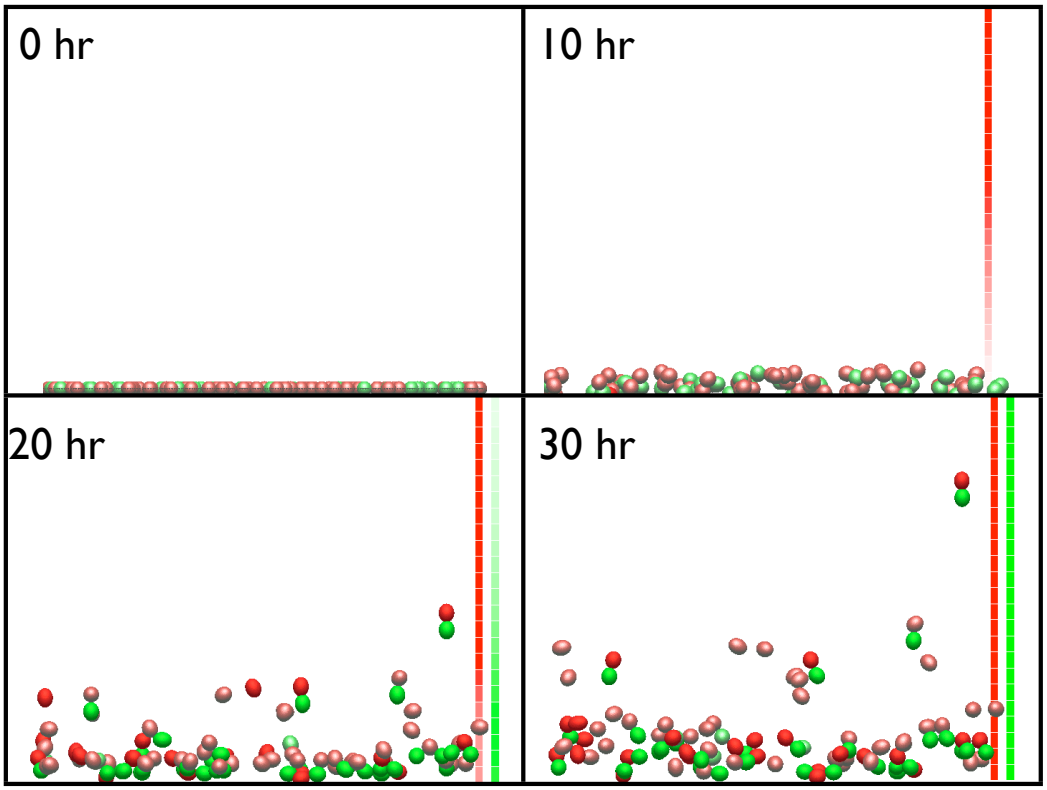

Figure 4.3: Snapshots at 4 different times, 0, 10, 20 and 30 hours. There was a CSF-1 gradient from the overlaid media. The macrophages moved in the direction of the CSF-1 gradient and the tumor cells followed them. Both cell types degraded both CSF-1 and EGF. When a cell changed to a brighter colour it indicated that it was chemotacting along a gradient. Approximately 28% of tumor cells and 38% of macrophages were invasive in this simulation. All parameters were as shown in Table 4.1.

70% of cells are macrophages; The concentration of CSF-1 in the media is 200 fold the threshold concentration (Table 4.1). The media containing CSF-1 is placed 500 μm above the cells. The simulation time is around 30 hours, which is comparable to the experimental time of 24 hours. These simulations resulted in an average of 23% invasive tumor cells and 31% invasive macrophages. Snapshots from one of these simulations can be seen in Figure 4.3 where 28% tumor cells and 38% macrophages were invasive. The invasive tumor cells follow closely behind invasive macrophages as was observed in the experiments and the two cell types seem to move in pairs. This individual cell based model allows for various other information to be acquired such as the average EGF and CSF-1 concentrations at different times in the simulation as well as the percentage of invasive cells as a function of time (Figure 4.4).

Parameter	**Value**	**Symbol**
CSF-1 MB degradation*	4 min^{-1}	k_{mem}^{csf}
EGF MB degradation*	1 min^{-1}	k_{mem}^{egf}
CSF-1 secretion*	0.02 nM/min	k_{sec}^{tumor}
EGF secretion*	0.03 nM/min	k_{sec}^{macro}
CSF-1 gradient threshold	0.1 nM	k_{thr}^{macro}
EGF gradient threshold	0.02 nM	k_{thr}^{tumor}
External CSF-1 concentration	10 nM	
Percentage of macrophages	70%	

Table 4.1: **Parameter values** - List of parameters used to generate a desired percentage of invasive tumor cells. MB: membrane-bound. *Note: these parameter values have been selected to fit this model, they should not be directly compared to parameters in other models or in experiments.

4.2 Membrane-bound degradation

In the simulation results in Figure 4.5, tumor cells degrade EGF and macrophages degrade CSF-1. I increased the CSF-1 membrane-bound degradation coefficient, with k_{mem}^{egf} = 1 min^{-1}, and investigated how it affected invasion of cells. The percentage of invasive macrophages had a biphasic response to increase in the CSF-1 membrane-bound degradation coefficient with a maximum value at k_{mem}^{csf} = 10 min^{-1}. Increasing the CSF-1 membrane-bound degradation coefficient sharpened the gradient of CSF-1 from the overlaid media, hence more macrophages chemotacted along the gradient. When $k_{mem}^{csf} > 10$ min^{-1} the degradation resulted in a sub-threshold concentration of CSF-1, thus fewer macrophages chemotact towards the overlaid media. For k_{mem}^{csf} below 3 min^{-1} more tumor cells were invasive than macrophages. Close observation showed that those invasive

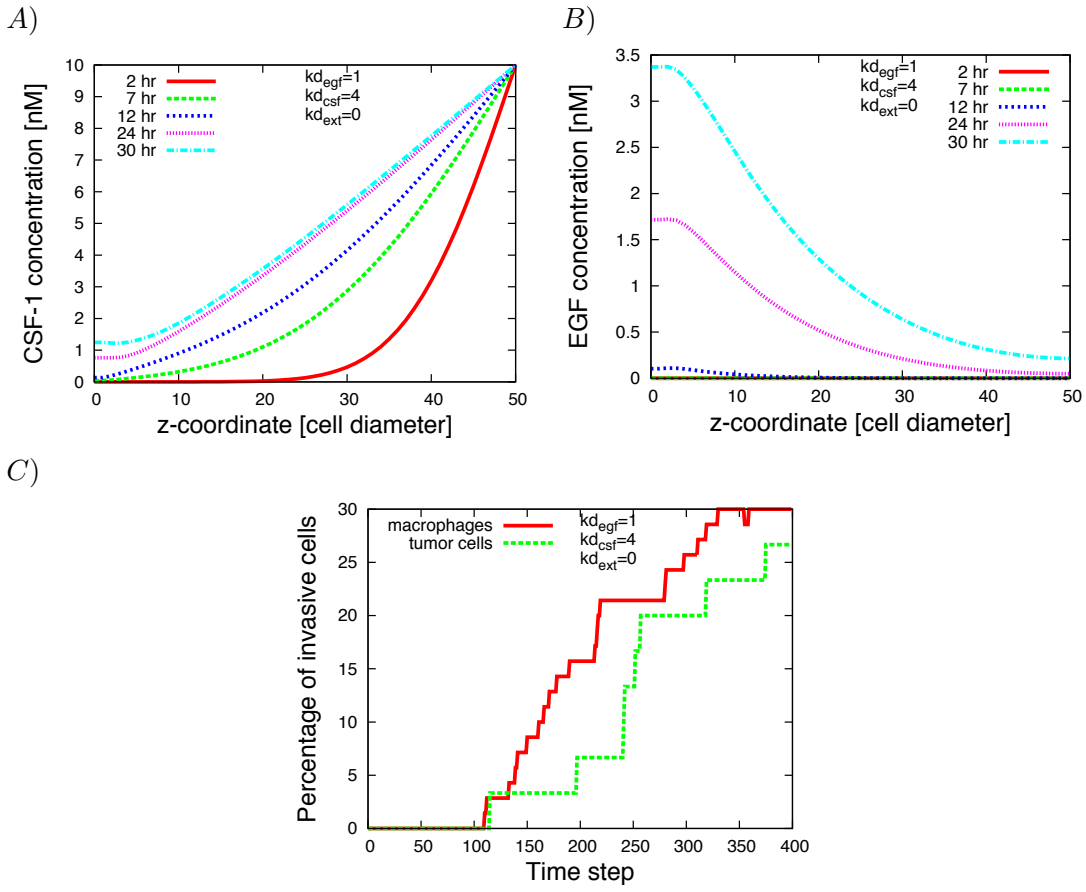

Figure 4.4: Results from one simulation where 27% of tumor cells became invasive. A) Average CSF-1 concentration at different times in the simulation. B) Average EGF concentration at different times in the simulation. Z-coordinate value is in number of cell diameters (10 μm). C) Percentage of invasive tumor cells and macrophages. One time step equals 5 min. The simulation time was 33 hours. All parameters from Table 4.1 were used.

tumor cells were being pushed by the macrophages. The tumor cells were secreting CSF-1, the macrophages chemotact along a CSF-1 gradient and thus migrated towards the tumor cells. There is no mechanism in the model that prevents the cells from pushing on one another. Therefore, the movement of the macrophages in the direction of the CSF-1 gradient from the tumor cells resulted in them pushing the tumor cells upwards. This pushing of the cells on one another does not seem to be observed in the Goswami experiments.

I increased the EGF membrane-bound degradation coefficient, with k_{mem}^{csf} = 4 min^{-1}, and investigated the effect it had on invasive tumor cells and macrophages. Increasing k_{mem}^{egf} resulted in a sub-threshold concentration of EGF and thus, a decrease in the percentage of invasive tumor cells (Figure 4.5.B). The percentage of invasive macrophages reached a minimum of 10% when k_{mem}^{egf} = 5 min^{-1}. Invasive tumor cells secrete CSF-1, that contributed to the CSF-1 gradient from the overlaid media. When fewer tumor cells were invasive there was a sub-threshold gradient of CSF-1 for some of the macrophages, therefore fewer macrophages were invasive. Also, for low EGF membrane-bound degradation there can be some tumor cells that secrete CSF-1 but do not chemotact into the collagen. This causes build up of CSF-1 at the plate and thus, chemotaxis failure for some macrophages. Increasing k_{mem}^{egf} past 5 min^{-1} increased the percentage of invasive macrophages. This suggests that when more EGF was degraded there was a sub-threshold concentration of EGF. Thus, the CSF-1 from the non-invasive tumor cells at the plate did not cause chemotaxis failure and more macrophages could migrate towards the CSF-1 gradient from the overlaid media.

In the next simulations macrophages and tumor cells degraded both EGF and CSF-1 (Figure 4.6). I changed the CSF-1 membrane-bound degradation coefficient, with k_{mem}^{egf} = 1 min^{-1}, and investigated the effect it had on invasiveness of cells. Increasing the k_{mem}^{csf} resulted in a biphasic curve for percentage of invasive tumor cells and macrophages (Figure 4.6.A). Invasive tumor cells reached a maximum of 70% when k_{mem}^{csf} = 15 min^{-1}. However, the percentage of invasive macrophages reached a maximum of 40% when k_{mem}^{csf} = 7 min^{-1}. The different inflection points for invasive tumor cells and macrophages is a result of the difference in sensitivity to gradient steepness, which will be discussed further in section 4.4. The increase in percentage of collected macrophages was a result of the CSF-1 membrane-bound degradation sharpening the gradient from the overlaid media. One way in which the gradient gets sharpened is by degrading the CSF-1 secreted by the tumor cells. The decrease in percentage of collected macrophages was caused by a sub-threshold concentration of CSF-1. Tumor cells chemotact towards an EGF gradient from macrophages and therefore, the percentage of collected tumor cells follows the same trend as the percentage of collected macrophages. For k_{mem}^{csf} above 50 min^{-1} the sub-threshold concentration of CSF-1 resulted in neither tumor cells

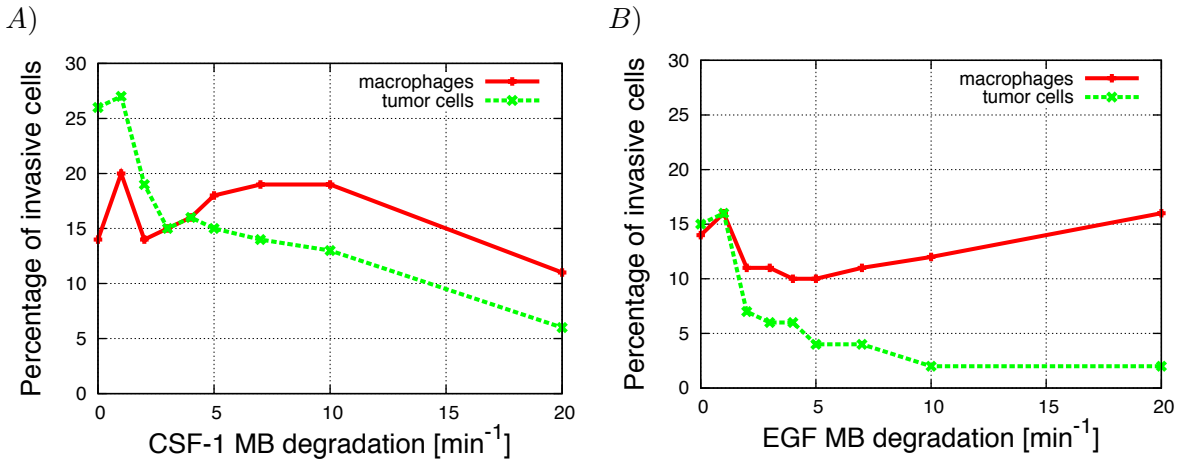

Figure 4.5: In these simulations tumor cells degraded EGF and macrophages degraded CSF-1 and there was no external degradation. A) Percentage of invasive macrophages and tumor cells as a function of k^{csf}_{mem}, with k^{egf}_{mem} = 1 min^{-1}. B) Percentage of invasive macrophages and tumor cells as a function of k^{egf}_{mem}, with k^{csf}_{mem} = 4 min^{-1}.

nor macrophages invading. For k^{csf}_{mem} below 2 min^{-1} around 30% of the tumor cells were invasive, however closer observation showed that those tumor cells were being pushed by the macrophages like in the previous scenario where only macrophages degraded CSF-1.

The percentage of invasive tumor cells in the simulations (Figure 4.6.A), can be compared to results from Goswami *et al.*'s experiments [21] with different cell lines. If the cells in the simulations had k^{csf}_{mem} = 4 min^{-1} then 23% of the tumor cells became invasive but if k^{csf}_{mem} = 10 min^{-1} then 71% of the tumor cells became invasive. In the experiments with MTLn3 cells, 25% of the tumor cells were observed to be invasive and in experiments with MDA-MB-231 cells 70% of the tumor cells were invasive. Based on my simulations, one possible hypothesis is that MTLn3 cells have a lower CSF-1 membrane-bound degradation than MDA-MB-231 cells.

I changed the membrane-bound degradation of EGF, with k^{csf}_{mem} = 4 min^{-1}, and investigated the effect it had on the percentage of invasive cells (Figure 4.6.B). The percentage of invasive macrophages increased with increasing EGF membrane-bound degradation coefficient. The secretion of CSF-1 by tumor cells could cause chemotaxis failure of macrophages. When k^{egf}_{mem} is increased some tumor cells experience a sub-threshold concentration of EGF resulting in reduced CSF-1 secretion. In turn, the lower secretion of CSF-1 reduced likelihood of chemotaxis failure and more macrophages migrated towards the CSF-1 gradient from the overlaid media. Increasing k^{egf}_{mem}

gives a biphasic curve for percentage of invasive tumor cells. The initial increase in invasive tumor cells was caused by the EGF membrane-bound degradation sharpening the EGF gradient from the macrophages as well as an increase in invasive macrophages. The decrease in invasive tumor cells was caused by a sub-threshold concentration of EGF from the macrophages. For $k_{mem}^{egf} > 20$ min^{-1} there were no invasive tumor cells.

Interestingly, these results suggest that by increasing the amount of EGF or CSF-1 degraded at the cell membrane the percentage of invasive tumor cells could be decreased and/or eliminated all together.

The two degradation scenarios explored here resulted in different trends when the CSF-1 and EGF membrane-bound degradation coefficients were altered. In the first scenario, when tumor cells degraded EGF and macrophages degraded CSF-1, the cells were observed to be pushing one another into the collagen, which is not the case in the experiments. In the second scenario, where EGF and CSF-1 were degraded by both cell types, the tumor cells migrated behind the macrophages in the direction of the overlaid media and the two cell types often moved in pairs. These simulations resemble the experimental results better. Hence, for the remainder of the simulations in this thesis both tumor cells and macrophages will degrade both EGF and CSF-1.

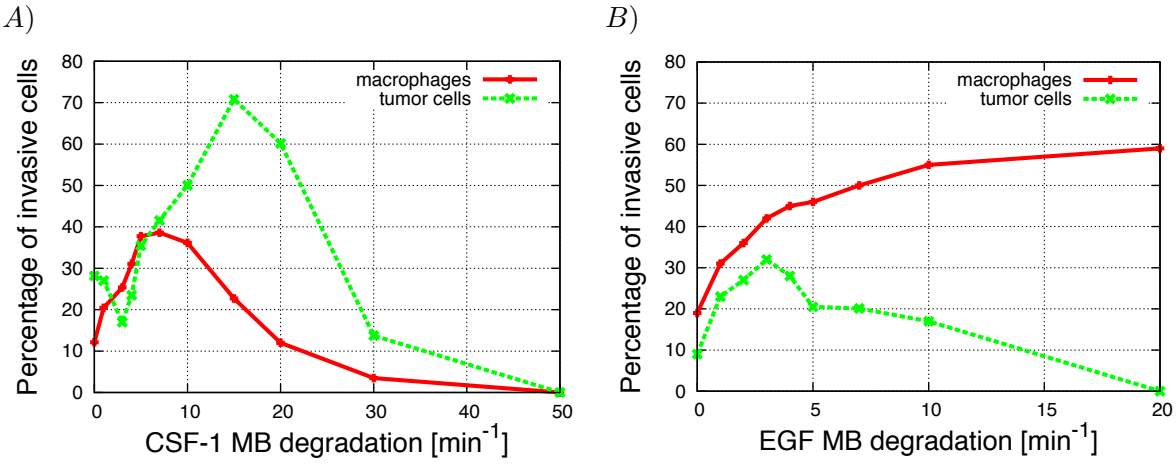

Figure 4.6: Tumor cells and macrophages degrade both CSF-1 and EGF. A) Percentage of invasive macrophages and tumor cells fas a function of k_{mem}^{csf}, with k_{mem}^{egf} = 1 min^{-1}. B) Percentage of invasive macrophages and tumor cells as a function of k_{mem}^{egf}, with k_{mem}^{csf} = 4 min^{-1}.

4.3 EGF and CSF-1 secretion

First, I investigate what happens when the secretion coefficient for CSF-1 by tumor cells is changed while keeping the EGF secretion coefficient by macrophages fixed. When the k_{sec}^{tumor} was increased, with k_{sec}^{macro} = 0.03 nM/min, the percentage of invasive tumor cells and macrophages had a sharp transition from a high to a low level (Figure 4.7.A). The decrease in invasive tumor cells hinged on the threshold value for detection in the model and at high k_{sec}^{tumor} chemotaxis failure of macrophages occurred. Fewer invasive macrophages resulted in a sub-threshold gradient of EGF and fewer tumor cells could follow the macrophages into the collagen.

These results can also be compared to experimental results from Goswami *et al.* [21] that show 25% invasive MTLn3 tumor cells and 70% invasive MDA-MB-231 tumor cells. In simulations, when k_{sec}^{tumor} = 0.0001nM/min, 68% of tumor cells were invasive and when k_{sec}^{tumor} = 0.03 nM/min, 23% tumor cells were invasive. Therefore, another possible explanation for the different percentage of invasive cells for these two cell lines is that they secrete different amounts of CSF-1. MDA-MB-231 cells might secrete more CSF-1 than MTLn3 cells.

In Figure 4.7.B, the EGF secretion by macrophages was changed, with k_{sec}^{tumor} = 0.02 nM/min, and the invasiveness of cells investigated. The percentage of invasive macrophages decreased with increasing k_{sec}^{macro}. Increasing k_{sec}^{macro} resulted in a higher EGF concentration which activated more tumor cells to secrete CSF-1. More tumor cells secreting CSF-1 caused chemotaxis failure of macrophages. The percentage of invasive tumor cells had a biphasic response to increasing secretion of EGF with a maximum value of 23% when k_{sec}^{macro} = 0.03 nM/min (Figure 4.7.B). If k_{sec}^{macro} was low, the EGF gradient was shallow, and for many of the tumor cells there was a sub-threshold gradient of EGF. When the k_{sec}^{macro} was increased the EGF gradient from the invasive macrophages became steeper and hence more tumor cells were invasive. The more interesting result is that the number of invasive tumor cells decreased for $k_{sec}^{macro} > 0.03$ nM/min. The number of invasive macrophages was decreasing in this region, therefore there were fewer tumor cells close enough to an invasive macrophage to detect a gradient of EGF above threshold and follow the invasive macrophages into the collagen.

These simulation results can be compared to results from Goswami *et al.*'s experiments [21] conducted with different macrophages. Figure 2.C in Goswami *et al.* [21] shows the percentage of invasive MTLn3 tumor cells when plated with either BAC or LR5 macrophages. When plated with BAC macrophages $\sim$25% of the tumor cells are invasive but when plated with LR5 macrophages only $\sim$15% tumor cells are invasive. In the simulation results in Figure 4.7.B, macrophages that

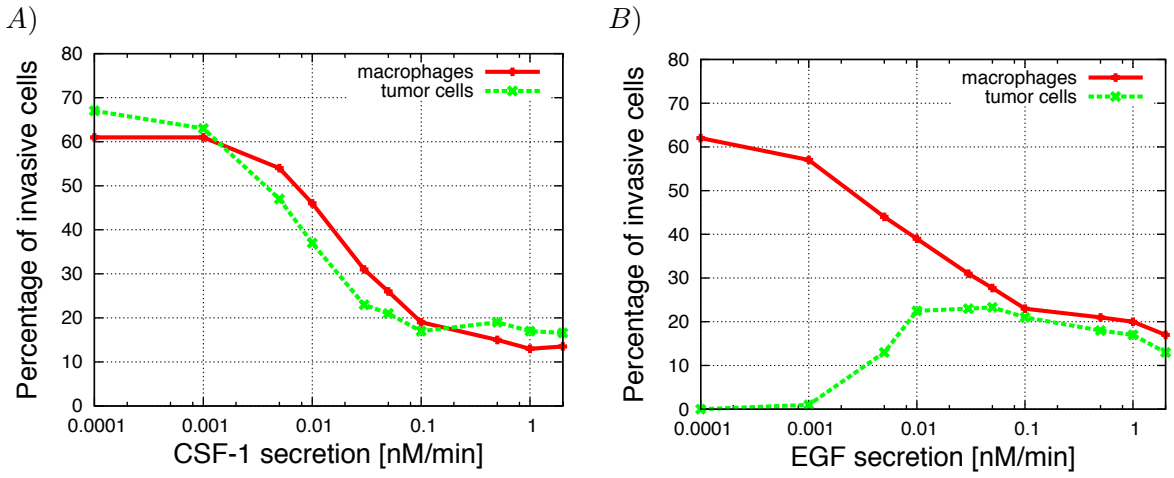

Figure 4.7: Tumor cells and macrophages degraded both EGF and CSF-1. A) Percentage of invasive macrophages and tumor cells as a function of CSF-1 secretion by tumor cells, with k_{sec}^{macro} = 0.03 nM/min. B) Percentage of invasive macrophages and tumor cells as a function of EGF secretion by macrophages, with k_{sec}^{tumor} = 0.02 nM/min.

secreted 0.005nM/min EGF promoted 12% invasive tumor cells whereas macrophages that secreted 0.03nM/min EGF promoted 22% invasive tumor cells. These results suggest that one possible difference between the two types of macrophages is that LR5 macrophages might secrete lower amounts of EGF than BAC macrophages.

4.4 Sensitivity to gradient steepness

The sensitivity to steepness of gradient varies between cell lines. Some cells can detect a difference in only a few bound receptors across their diameter. Here, I investigate how the percentage of invasive tumor cells and macrophages was altered when sensitivity to the gradient steepness of either EGF or CSF-1 was changed. Decreasing a cells sensitivity to a gradient steepness corresponds to increasing the gradient threshold value for detection in the model.

Increasing the CSF-1 gradient threshold, with k_{thr}^{tumor} = 0.02 nM, decreased the percentage of invasive macrophages. This was to be expected because increasing the CSF-1 gradient threshold meant that the CSF-1 gradient from the overlaid media needed to be steeper for the macrophages to chemotact along the gradient. Therefore, there was a sub-threshold gradient of CSF-1 for more

macrophages when k_{thr}^{macro} was increased. The percentage of invasive tumor cells had a biphasic response to increasing CSF-1 gradient threshold with a minimum of 23% when k_{thr}^{macro} = 0.1 nM (meaning that a 0.1 nM difference in concentration was needed across the cell diameter) (Figure 4.8.A). The initial decrease in invasive tumor cells was a result of fewer invasive macrophages and thus a subthrehsold gradient of EGF. Counterintuitively, the invasive tumor cells did not follow the decreasing trend of the invasive macrophages for $k_{thr}^{macro} > 0.1$ nM, but rather increased. One possible explanations is that for high k_{thr}^{macro} the macrophages secreted EGF before becoming invasive. The tumor cells can chemotact towards the EGF gradient from the macrophages at the bottom. Thus, the delayed invasive response of the macrophages enabled the tumor cells to migrate closer to the macrophages before the macrophages got out of range.

When the threshold value for detection of EGF gradient was increased, with k_{thr}^{macro} = 0.1 nM, the percentage of invasive tumor cells and macrophages decreased (Figure 4.8.B). Increasing the EGF gradient threshold implies that the EGF gradient from the macrophages needed to be steeper for the tumor cells to chemotact along the gradient. Therefore, increasing the EGF gradient threshold resulted in a sub-threshold gradient of EGF for more tumor cells. The increased EGF gradient threshold had a very slight effect on the percentage of invasive macrophages. The slight decrease in the percentage of invasive macrophages was due to the decrease in percentage of invasive tumor cells. The decrease in invasive tumor cells increases the number of macrophages that encounter a sub-threshold gradient of CSF-1.

4.5 External CSF-1 concentration

The concentration of CSF-1 in the media above the collagen was not given in Goswami *et al.* [21]. I therefore investigated how changing the amount of external CSF-1 in the model affected the percentage of invasive cells. The simulations showed that when the external CSF-1 concentration was increased, the percentage of invasive tumor cells and macrophages increased (Figure 4.9). These results are not surprising because a higher external CSF-1 concentration resulted in a steeper gradient from the overlaid media and more macrophages became invasive. Tumor cells can migrate along a gradient of EGF secreted by macrophages, therefore when the number of invasive macrophages increased that resulted in increasing number of invasive tumor cells. The increase in number of invasive macrophages enhanced the chances of a tumor cell being close enough to an invasive macrophage to detect a gradient of EGF above threshold, therefore more tumor cells became invasive. The attenuating effect that the CSF-1 secretion by the tumor cells located at the plate had on

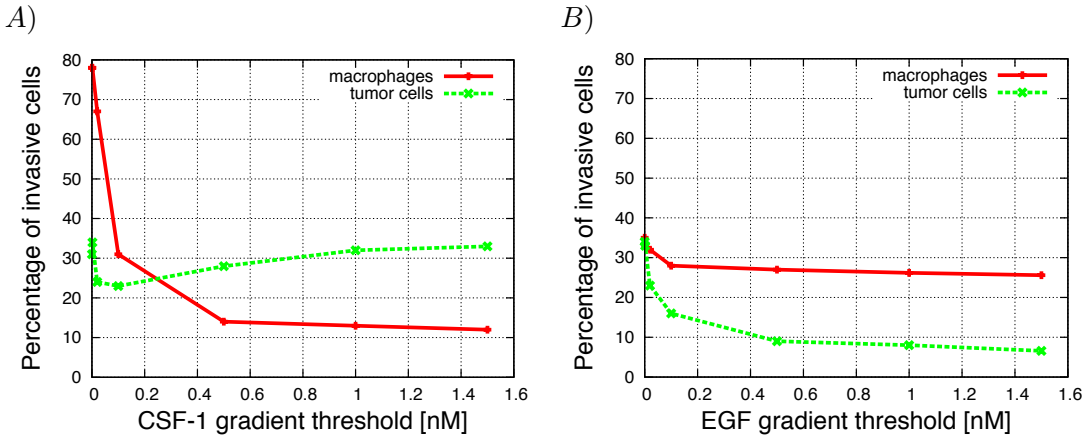

Figure 4.8: A) Percentage of invasive macrophages and tumor cell as a function of CSF-1 gradient threshold, with k_{thr}^{tumor} = 0.02 nM. B) Percentage of invasive macrophages and tumor cell as a function of EGF gradient threshold, with k_{thr}^{macro} = 0.1 nM.

the CSF-1 gradient from the overlaid media became less significant when the CSF-1 concentration in the media was higher. In the simulations, all of the cells could chemotact along a gradient if it was above the threshold value for detection set in the model. Note that in experiments this might not be the case. If the cell culture contains a mixture of Mena11a and Mean^{INV} cells, as discussed in chapter 1.2, then the Mena11a cells are unlikely to chemotact along a gradient.

4.6 Ratio of macrophages to tumor cells

It is of interest to change the initial ratio between tumor cells and macrophages because it is not the same in all patients and it can also differ within a tumor. The initial ratio can easily be changed in the simulations which can alter invasiveness of cells. The simulation results could be checked by repeating the experiments by Goswami *et al.* [21] with different initial ratios of macrophages to tumor cells.

In these simulations, the percentage of invasive tumor cells reached a minimum value of 23% when 70% of total cells were macrophages. The percentage of invasive macrophages had a similar trend but with a minimum value of 30% which was reached when 60% of the cells in the initial culture were macrophages (Figure 4.10.B). These trends can be more easily explained and understood when looking at the number of invasive tumor cells and macrophages. The number of invasive

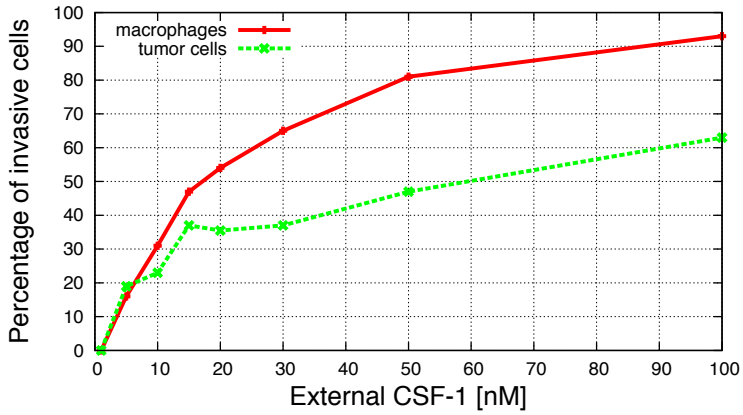

Figure 4.9: Percentage of invasive macrophages and tumor cells as a function of external concentration of CSF-1. All other parameter values as in Table 4.1.

tumor cells decreased when the percentage of macrophages in the initial culture increased (fewer tumor cells in the simulations). Fewer tumor cells were close enough to invading macrophages to detect a gradient of EGF above threshold and to follow the invading macrophages into the collagen. When the percentage of macrophages in the initial culture was increased the number of invasive macrophages increased. Fewer tumor cells in the simulations resulted in a decrease in CSF-1 concentration at the plate and fewer macrophages encountered chemotaxis failure.

4.7 Summary

In this chapter, I explored the parameter space to observe the effect that each parameter had on the percentage of invasive tumor cells and macrophages. The results are summarized in Table 4.2. This sensitivity analysis enhances our understanding of the function of each of the model parameters in the paracrine signaling pathway. Changing some of the model parameters could eliminate the invasive tumor cells which is one of the objectives in cancer treatments.

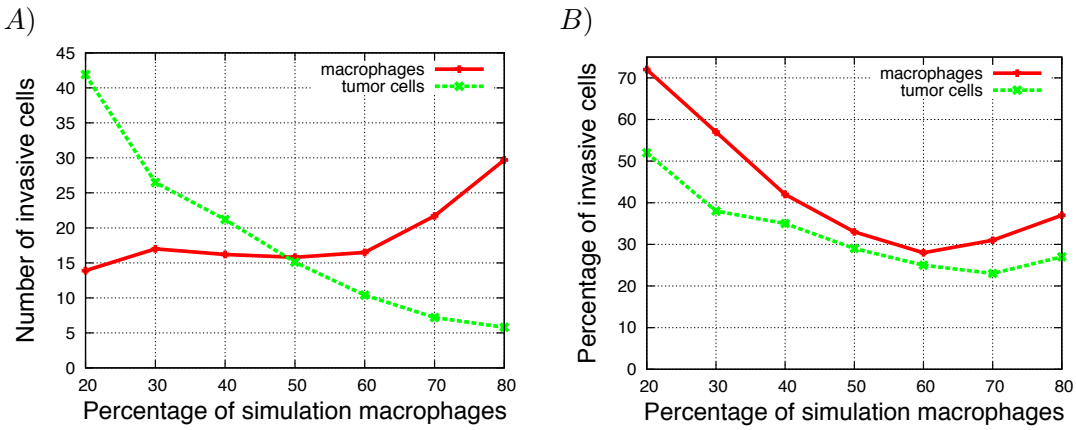

Figure 4.10: Tumor cells and macrophages degraded both CSF-1 and EGF. A) The average number of invasive cells for different percentage of macrophages in the initial culture. B) The average percentage of invasive cells for different percentage of macrophages in the initial culture.

Increase parameter	**Effect on invasive tumor cells**	**Effect on invasive macrophages**
CSF-1 degradation	Maxima	Maxima
EGF degradation	Maxima	Increases
CSF-1 secretion	Decreases	Decreases
EGF secretion	Maxima	Decreases
External CSF-1	Increases	Increases
CSF-1 slope thresh.	Minima	Decreases
EGF slope threshold	Decreases	Decreases
Ratio of macrophages	Decreases	Increases

Table 4.2: ***In vitro* simulation results** - This table lists the parameters that are varied in the simulations. The results are more sensitive to changes in some parameters than others. The second column shows how increasing that parameter value affects the number of invasive tumor cells. The third column shows how increasing that parameter value affects the number of invasive macrophages.

Chapter 5

Results from simulations of *in vivo* experiments

The previous chapter demonstrated how my model could be used to reproduce results from the *in vitro* experiments first described in chapter 2.1. In this chapter, I will use the same model to simulate the *in vivo* experiments conducted by Wyckoff *et al.* [22] and described in chapter 2.2. The experiments were conducted using mice with PyMT-induced mammary tumors. Micro-needles containing 25 nM of either EGF or CSF-1 were used to collect cells that migrated along the gradient from the needle. The needles were placed approximately 50 μm away from the tumor margin (Figure 2.2). Out of the 1,000 cells collected, approximately 73% were tumor cells and 26% were macrophages, giving a ratio of about 3 tumor cells to 1 macrophage.

To explain the motility behaviours in these simulations I will define two new phenomena:

- **Collected cells:** Cells that have migrated into the micro-needle in the simulations.
- **Paracrine enhancement:** The paracrine signaling loop can enhance the motility of cells. The macrophages secrete EGF that contributes to the EGF gradient from the needle. When more macrophages chemotact towards the needle the EGF gradient becomes steeper and thus more tumor cells are attracted towards the needle.

The parameters used in the simulations are listed in Table 5.1. I simulated the in *vivo* experiments by depositing cells at the bottom which represents the tumor margin. On top of the cells there is a collagen rich extracellular matrix in which the cells can move. In the centre of the extracellular matrix I placed a sphere representing the needle opening. Both EGF and CSF-1 can diffuse from this

sphere and cells can enter it and either be stored or removed. I also included external degradation of both EGF and CSF-1 to account for degradation and perfusion in the extracellular matrix. The membrane-bound degradation coefficients, the external chemical concentration and the percentage of macrophages were different from the values used to simulate the *in vitro* experiments.

Parameter	**Value**
External degradation*	0.02 min^{-1}
CSF-1 MB degradation*	1 min^{-1}
EGF MB degradation*	4 min^{-1}
CSF-1 secretion*	0.02 nM/min
EGF secretion*	0.03 nM/min
CSF-1 gradient threshold	0.1 nM
EGF gradient threshold	0.02 nM
EGF in needle	20 nM
Percentage of macrophages	40%
Percentage of motile cells	40%

Table 5.1: **Parameter values** - List of parameters used in simulations to generate a desired ratio of 3 tumor cells to 1 macrophage collected in a needle containing EGF. MB: membrane-bound. *Note: these parameter values have been selected to fit this model, they should not be directly compared to parameters in other models or in experiments.

In these simulations there were 1600 cells, approximately 40% of which were motile. Of the motile cells 40% were macrophages and 60% were tumor cells. I chose this ratio to simulate the tumor margin where there is a high density of macrophages [6]. The needle opening was represented by a black sphere with diameter two times the diameter of the cells. It was located 6 cell diameters above the cells in the centre of the x-y plane (Figure 5.1). In these simulations, in addition to the tumor cells and macrophages, there are grey cells that represent non-motile cells.

5.1 Collection needle containing EGF

In the following simulations (unless otherwise stated) the collection needle contained EGF. The diffusion profile of EGF can be seen in Figure 5.2. The z-axis represents the concentration of EGF at a given x- and y-coordinate averaged over the height. In all the simulations in this chapter, macrophages and tumor cells degraded both EGF and CSF-1. Once a cell touched the needle, it was no longer visible in the simulation but it could continue to secrete a signaling molecule for 40 min (EGF if it was a macrophage or CSF-1 if it was a tumor cell). As in the previous chapter, I explored the parameter space and investigated how the ratio of collected tumor cells to macrophages changed

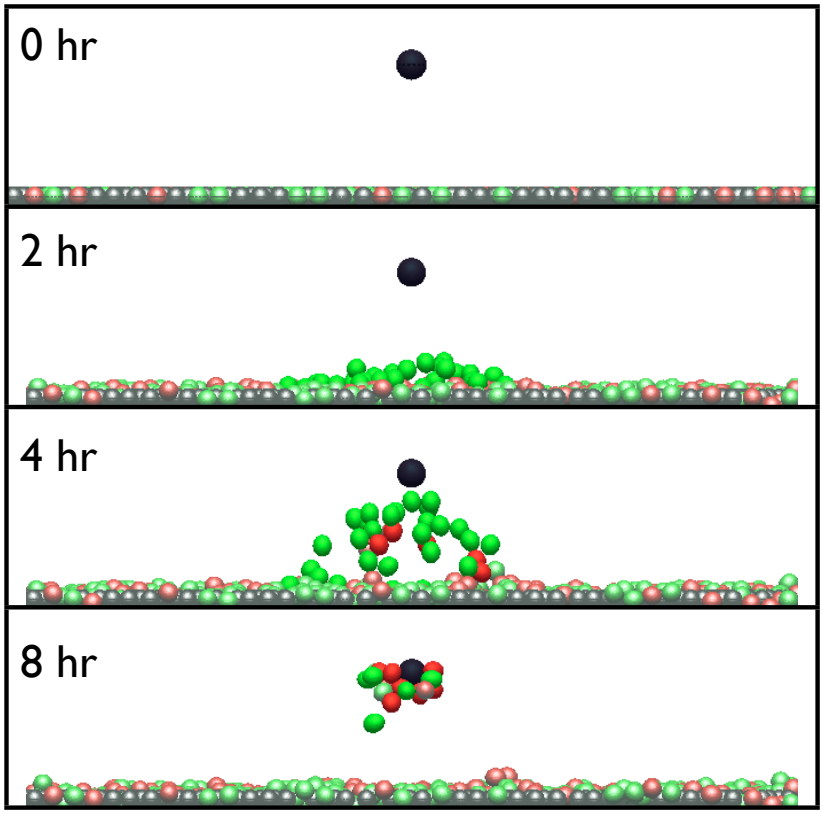

Figure 5.1: Four snapshots from an *in vivo* simulation after 0, 2, 4 and 8 hours. Green cells are tumor cells, red cells are macrophages, grey cells are immobile cells and the black circle represents the needle opening. Once a cell touches the needle it is no longer visible in the simulation. However, a cell that is located inside the needle can still secrete either EGF (for macrophages) or CSF-1 (for tumor cells).

when simulation parameters were altered. All values in the graphs were averaged over 50 differently randomized simulations and the 97.5% confidence intervals for the ratio of collected tumor cells to macrophages was displayed as error bars.

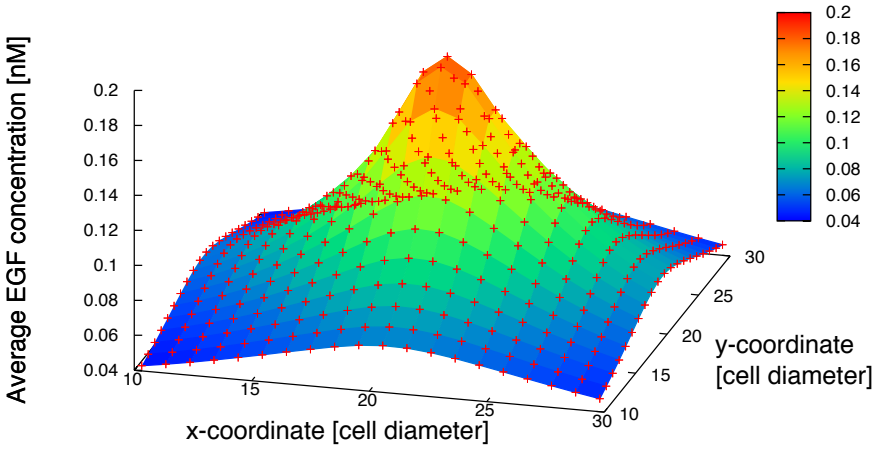

Figure 5.2: The needle contained EGF. It was located 6 cell diameters above the cells and in the centre of the x-y plane. This plot shows the EGF concentration (in nM) averaged over the height. The x- and y- coordinates are in number of cell diameters (10μm).

5.2 External degradation

In the simulations of the *in vivo* experiments, external degradation of both EGF and CSF-1 as well as membrane-bound degradation took place.

Increasing external degradation of both EGF and CSF-1 lead to a decrease in the number of collected tumor cells and macrophages, while the ratio of collected tumor cells to macrophages increased (Figure 5.3). This was to be expected because the external degradation caused a sub-threshold gradient of EGF for some of the tumor cells. The decrease in the number of collected tumor cells also resulted in a sub-threshold gradient of CSF-1 from the migrating tumor cells and thus a decrease in the number of collected macrophages.

The increase in the ratio of collected tumor cells to macrophages was caused by a combination of factors, (1) increasing external degradation caused a sub-threshold gradient of CSF-1 for some macrophages, (2) decreasing number of invasive tumor cells also resulted in a sub-threshold gradient of CSF-1, (3) when only a few tumor cells were invasive chances are there were no macrophages in

the vicinity of the invasive tumor cells that could follow them into the needle . Hence, the number of collected macrophages decreased faster than the number of collected tumor cells and the ratio increased.

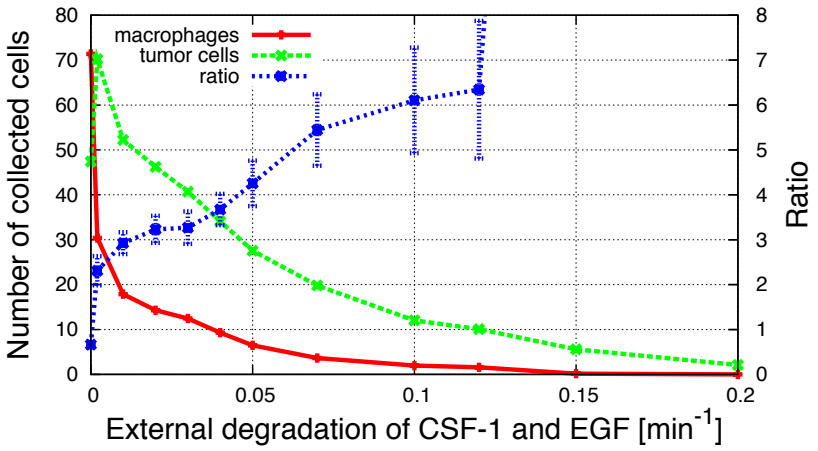

Figure 5.3: The external degradation coefficient of EGF and CSF-1 was increased while keeping all other parameters the same as in Table 5.1. The red and green lines show the number of collected macrophages and tumor cells, respectively (left y-axis). The blue line shows the ratio of collected tumor cells to macrophages (right y-axis) with 95% confidence interval. Each data point is an average from 50 different simulations.

5.3 Membrane-bound degradation

In addition to the external degradation the model also included membrane-bound degradation i.e. tumor cells and macrophages degraded both EGF and CSF-1. Here, the external degradation coefficient of EGF and CSF-1 was kept fixed at 0.02 min^{-1}.

I changed the CSF-1 membrane-bound degradation coefficient, with k_{mem}^{egf} = 4 min^{-1}, and investigated the effect it had on the collected cells. When there was no membrane-bound CSF-1 degradation, fewer tumor cells and macrophages were collected than when k_{mem}^{csf} = 1 min^{-1} (Figure 5.4.A). Figure 5.5 shows the average CSF-1 concentration at different times in simulations for A) no CSF-1 membrane-bound degradation and B) k_{mem}^{csf} = 1 min^{-1}. In A) the concentration of CSF-1 at the tumor margin was building up resulting in chemotaxis failure of macrophages whereas in B) the

degradation made the gradient sharper and more cells were invasive. Further increasing the CSF-1 membrane-bound degradation decreased the number of collected tumor cells and macrophages which is logical because it resulted in sub-threshold concentration of CSF-1 for some macrophages. The number of collected tumor cell decreased as well because there was less paracrine enhancement. There was only a slight decrease in the number of collected tumor cells when the CSF-1 membrane-bound degradation coefficient was increased whereas the number of collected macrophages went to zero. Hence, the ratio of collected tumor cells to macrophages increased with increasing CSF-1 membrane-bound degradation coefficient.

Simulations with no EGF membrane-bound degradation were compared to simulations with k_{mem}^{egf} = 1 min^{-1}. The same effect on the number of collected cells was observed as in the previous paragraph when comparing the two scenarios for changes in CSF-1 membrane-bound degradation. Further increasing the EGF membrane-bound degradation coefficient decreased the number of collected tumor cells because of a sub-threshold concentration of EGF. When the number of collected tumor cells decreased that resulted in a sub-threshold gradient of CSF-1 for some macrophages (Figure 5.4.B). When $k_{mem}^{egf} > 30$ min^{-1} the sub-threshold concentration of EGF resulted in no cells being collected.

The ratio of tumor cells to macrophages stayed around 3, within the error margins, for EGF membrane-bound degradation between 1 and 15 min^{-1}, which suggested that the number of collected tumor cells and macrophages decreased proportionally. For $k_{mem}^{egf} > 15$ min^{-1} there was a subtheshold concentration of EGF for some tumor cells that impacted the CSF-1 concentration. The combination of the sub-threshold gradient of CSF-1 and the sub-threshold concentration of EGF resulted in the number of collected macrophages decreasing more than the number of collected tumor cells, thus the ratio of collected tumor cells to macrophages increased.

Comparing Figures 5.4.A and B, showed that the CSF-1 membrane-bound degradation coefficient had a greater effect on the ratio of collected tumor cells to macrophages than the EGF membrane-bound degradation coefficient (notice the different scales of the right y-axis for the two figures). For EGF membrane-bound degradation coefficient between 1 and 15 min^{-1} the ratio of collected tumor cells to macrophages stayed around 3. Changing the CSF-1 membrane-bound degradation coefficient from 1 to 5 min^{-1} changed the ratio from 3 to 15. Hence, the ratio seemed to be more sensitive to changes in CSF-1 membrane-bound degradation than to changes in EGF membrane-bound degradation. However, not surprisingly, the number of collected tumor cells was more sensitive to changes in EGF membrane-bound degradation than CSF-1 membrane-bound degradation. Increasing the EGF membrane bound degradation coefficient could eliminate the number of invasive

cells.

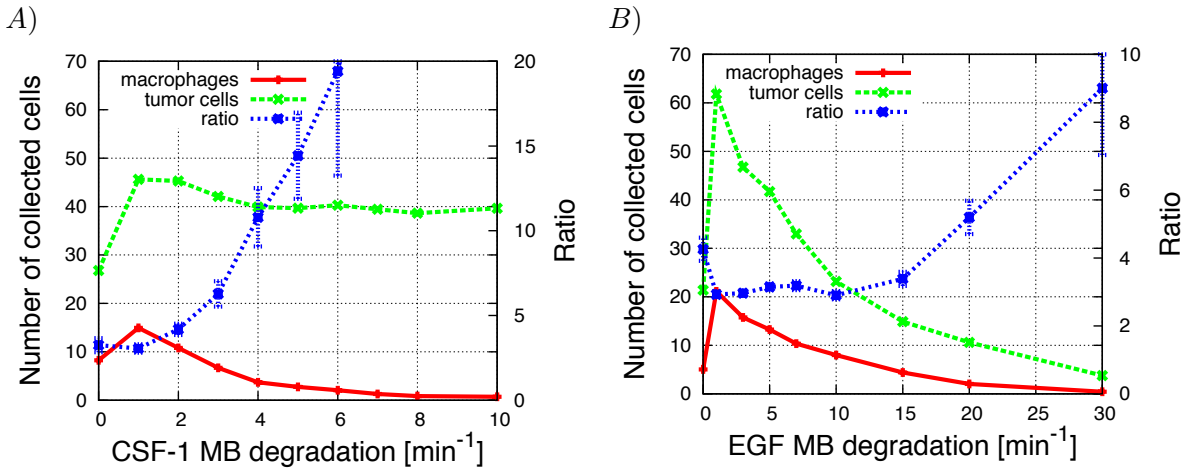

Figure 5.4: A) Number of collected tumor cells and macrophages as well as the ratio of collected tumor cells to macrophages as a function of CSF-1 membrane-bound degradation coefficient, with k_{mem}^{egf} = 4 min^{-1}. B) Number of collected tumor cells and macrophages as well as the ratio of collected tumor cells to macrophages as a function of EGF membrane-bound degradation coefficient, with k_{mem}^{csf} = 1 min^{-1}. Notice the different scale of the right y-axis of the two graphs.

5.4 EGF and CSF-1 secretion

I changed the secretion coefficients, for EGF and CSF-1, in the model and investigated how it affected the number and ratio of collected cells. Increasing the CSF-1 secretion coefficient, with k_{sec}^{egf} = 0.03 nM/min, resulted in a biphasic curve for the number of collected tumor cells with a maximum at k_{sec}^{csf} = 0.03 nM/min (Figure 5.6.A). The number of collected tumor cells initially increased because of the paracrine enhancement. When $k_{sec}^{csf} > 0.02$ nM/min the increasing concentration of CSF-1 activated more macrophages to secrete EGF. The increased secretion of EGF resulted in chemotaxis failure by some of the tumor cells. The number of collected macrophages had the same biphasic curve when k_{sec}^{csf} was increased but had an inflection point at k_{sec}^{csf} = 0.1 nM/min. The initial increase in collected macrophages was due to the increasing CSF-1 secretion by collected tumor cells resulting in a gradient with a steepness above the threshold value. The later decrease in collected macrophages was a result of fewer collected tumor cells and thus a sub-threshold gradient of CSF-1.

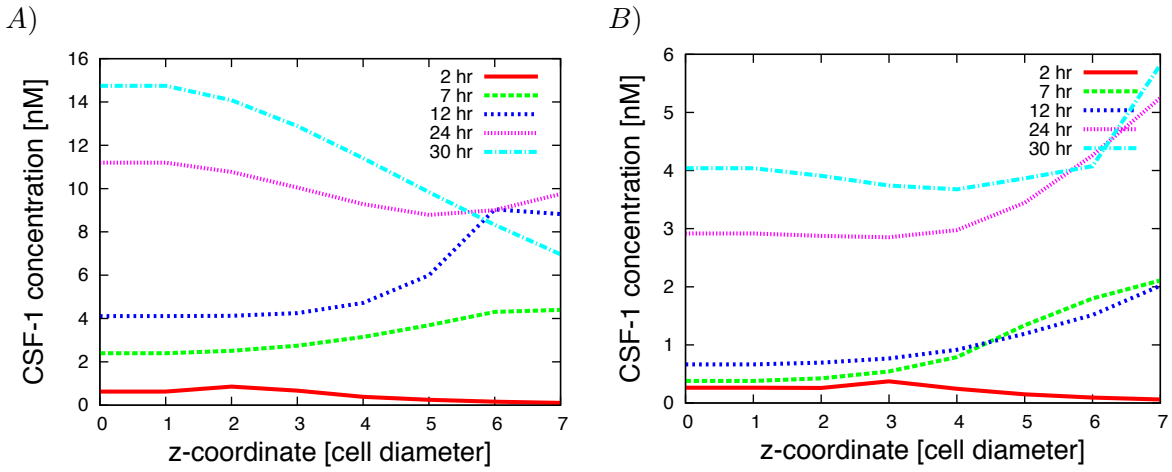

Figure 5.5: A) Average CSF-1 concentration for k_{mem}^{csf} = 0 min^{-1} and k_{mem}^{egf} = 4 min^{-1}. The needle was located at z=7. The z-coordinate is in number of cell diameters (10 μm). B) Average CSF-1 concentration for k_{mem}^{csf} = 1 min^{-1} and k_{mem}^{egf} = 4 min^{-1}.

The ratio of collected tumor cells to macrophages initially decreased when the CSF-1 secretion coefficient was increased. The decrease in ratio was a result of more macrophages chemotacting towards a now steeper CSF-1 gradient. For $k_{sec}^{csf} > 0.1$ nM/min the ratio was constant at around 2, within error margins. The constant ratio indicates that the macrophages reached their full chemotactic potential and the collected macrophages decreased proportionally to the decrease in collected tumor cells.

Increasing the EGF secretion coefficient for macrophages, with k_{sec}^{tumor} = 0.02 nM/min, resulted in biphasic curves for the number of collected tumor cells and macrophages. The number of collected tumor cells and macrophages both had a maximum value when the k_{sec}^{macro} = 0.02 nM/min (Figure 5.6.B). For $k_{sec}^{macro} > 1$ nM/min no cells were collected. The number of collected macrophages followed the same trend as the number of collected tumor cells because the macrophages were chemotacting towards a CSF-1 gradient from the tumor cells. Changing the EGF secretion coefficient did not directly affect the CSF-1 gradient but it did so indirectly by changing the movement and secretion of CSF-1 from tumor cells. The increase in number of collected tumor cells was driven by the paracrine enhancement and was enhanced with more EGF secretion from the macrophages. The decrease in number of collected tumor cells was caused by chemotaxis failure of tumor cells. I explored this in more detail by looking at the time when cells were collected for two

different simulations, (i) k_{sec}^{macro} = 0.02 nM/min and (ii) k_{sec}^{macro} = 0.1 nM/min (Figure 5.7). Initially, the collection of cells in the two simulations was almost identical. However, after 200 time steps no more cells were collected in simulation (ii) whereas the number of collected cells kept increasing for simulation (i). The concentration profile of EGF, averaged over the y-coordinate, after 30 hours of simulation time are shown for (i) in Figure 5.8.A and (ii) in Figure 5.8.B. These results support my argument that the higher EGF secretion coefficient resulted in chemotaxis failure.

For low EGF secretion coefficient the ratio of tumor cells to macrophages remained constant within the error margin at a value of 3. It was only when the EGF secretion coefficient was increased past 0.02 nM/min that the ratio increased. The number of collected macrophages decreased because of (1) decreasing number of collected tumor cells and (2) chemotaxis failure. The chemotaxis failure by tumor cells results in some tumor cells at the tumor margin secreting CSF-1 that has an attenuating effect on the CSF-1 gradient from the invasive tumor cells. Thus, the chemotaxis failure of tumor cells causes fewer macrophages to be collected. The number of collected macrophages decreased faster than the number of collected tumor cells and therefore, the ratio of collected tumor cells to macrophages increased.

Figures 5.6.A and B show that changing the EGF or CSF-1 secretion coefficients could alter the number of collected tumor cells and macrophages significantly. Increasing secretion of either EGF or CSF-1 may prevent tumor cells from invading. When the EGF secretion coefficient was above 1 nM/min no cells were collected (Figures 5.6.B). However, changing these secretion coefficients did not have as great an effect on the ratio between collected tumor cells and macrophages as it did on the number of collected cells. When more than 10 cells of each type were collected, the ratio stays between 2 and 3.

5.5 Sensitivity to gradient steepness

Different cell lines have different sensitivities to gradient steepness as described in the previous chapter. In this section, I systematically decreased the sensitivity of the cells to gradient steepness and investigated how the number of collected cells changed. Decreasing the sensitivity of a cell to gradient steepness corresponds to increasing the gradient threshold.

Increasing the CSF-1 gradient threshold for the macrophages, with $\nabla[E]_{th}$ = 0.02 nM, decreased the number of collected tumor cells and macrophages (Figure 5.9.A). When the CSF-1 gradient threshold was above 1 nM (meaning a 1 nM change in concentration across the cell diameter) no macrophages were collected. The decrease in the number of collected macrophages was a result of a

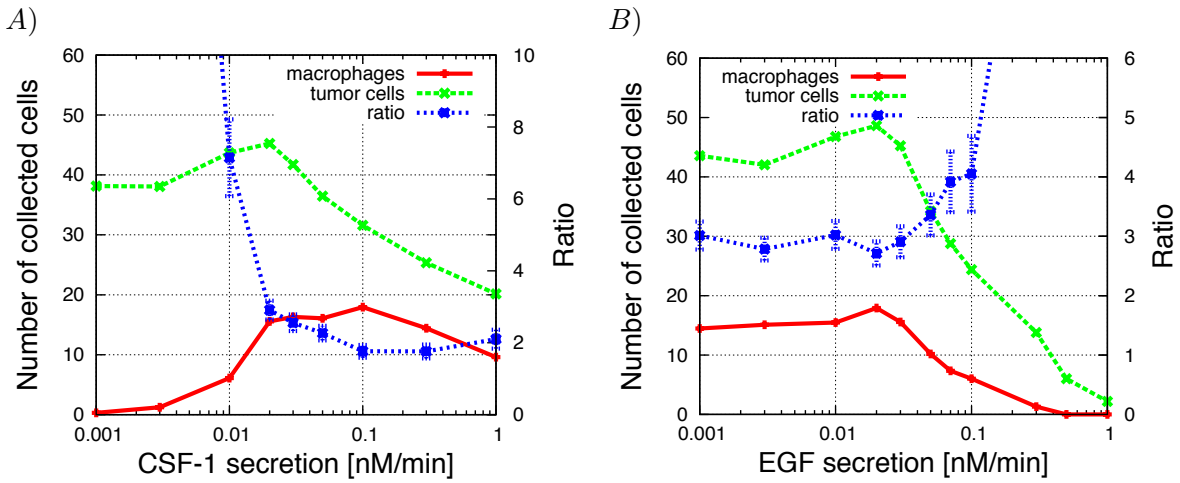

Figure 5.6: A) Collected tumor cells and macrophages as well as the ratio between collected tumor cells and macrophages as a function of CSF-1 secretion by the tumor, k_{sec}^{egf} = 0.03 nM/min. B) shows the same quantities but as a function of EGF secretion by macrophages where k_{sec}^{csf} = 0.02 nM/min. Notice that the two right y-axises have different scales.

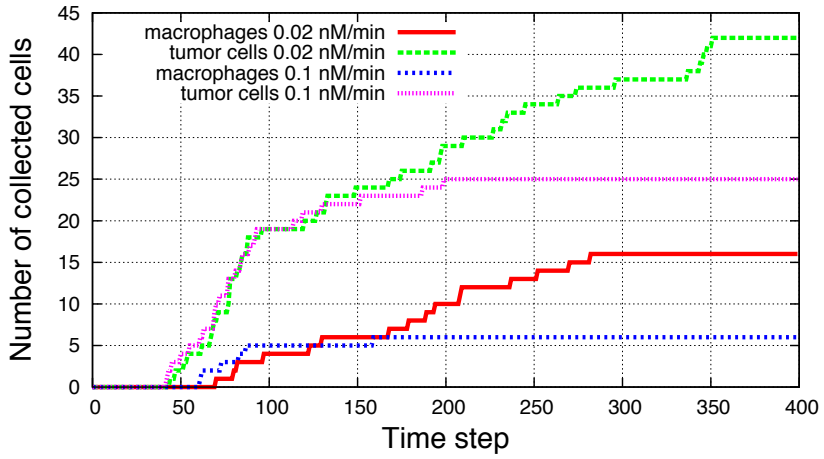

Figure 5.7: The time at which the tumor cells and macrophages were collected for two different simulations with k_{sec}^{egf} = 0.02 nM/min (red and green lines) and k_{sec}^{egf} = 0.1 nM/min (blue and pink lines). For the first 150 time steps the number of collected cells was almost the same. After 200 time steps the simulation with k_{sec}^{egf} = 0.1 nM/min had no additional tumor cells or macrophages collected while the number of collected cells in simulation with k_{sec}^{egf} = 0.02 nM/min kept on increasing. Each time step was 5 min.

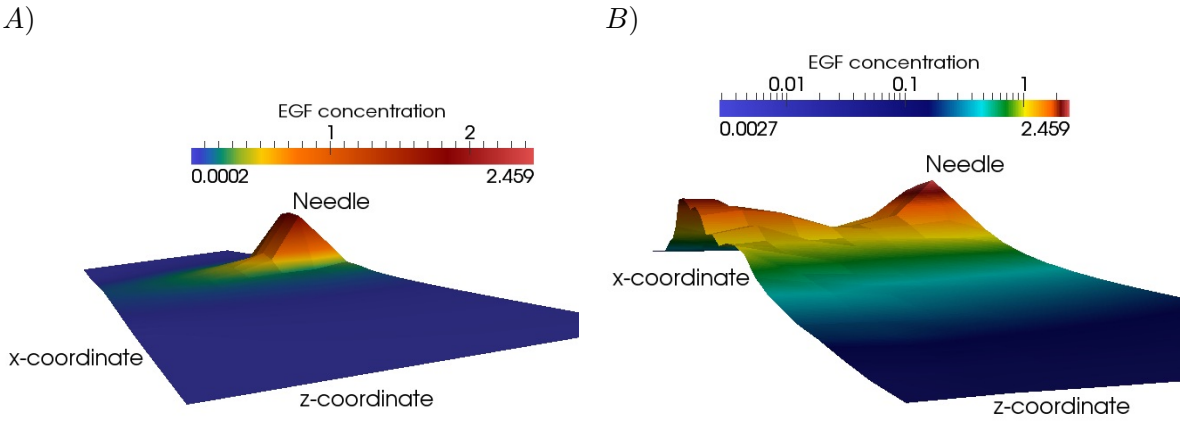

Figure 5.8: The EGF concentration profile averaged over the y-coordinate for A) k_{sec}^{egf} = 0.02 nM/min and B) k_{sec}^{egf} = 0.1 nM/min after 30 hours in the simulation. In A) there was a gradient towards the needle that the cells could chemotact towards. In B) there was a build up of EGF at the tumor margin (z-coordinate = 0) that resulted in chemotaxis failure.

sub-threshold gradient of CSF-1 for some of the macrophages. The number of collected tumor cells decreased slightly when the CSF-1 gradient threshold was increased, a demonstration of the lack of paracrine enhancement. When the CSF-1 gradient threshold was below 0.1 nM the ratio between collected tumor cells and macrophages was constant around 2, within error margins. Increasing the CSF-1 gradient threshold past 0.1 nM resulted in an increase in the ratio of collected tumor cells to macrophages. Changing the sensitivity of macrophages to gradients of CSF-1 had a greater effect on the number of collected macrophages than the number of collected tumor cells, as was to be expected.

Increasing the EGF gradient threshold, with $\nabla[C]_{th}$ = 0.1 nM, lead to a decrease in the number of collected tumor cells and macrophages (Figure 5.9.B). The number of collected tumor cells decreased because now more tumor cells experienced a sub-threshold gradient of EGF. The decrease in collected tumor cells resulted in a sub-threshold gradient of CSF-1 from the collected tumor cells and thus a decrease in collected macrophages as well. For $\nabla[E]_{th} > 1$ nM the sub-threshold gradient of EGF resulted in no cells being collected. The ratio of collected tumor cells to macrophages only varied slightly with increasing EGF gradient threshold. The change in ratio when $\nabla[E]_{th} >$ 0.1 nM was caused by the different gradient threshold values for the two cell types.

In comparing Figures 5.9.A and B, the CSF-1 gradient threshold seemed to have a greater effect

on the ratio of collected tumor cells to macrophages than on the number of invasive tumor cells. The EGF gradient threshold, on the other hand, had a greater effect on the number of collected tumor cells than the ratio of collected tumor cells to macrophages. Increasing $\nabla[E]_{th}$ could eliminate the number of collected cells because the needle contained EGF and therefore if $\nabla[E]_{th}$ was too high no tumor cells migrate into the needle. Macrophages migrate following a gradient of CSF-1 from the tumor cells, therefore no macrophages migrate into the needle when no tumor cells migrate into the needle. The ratio on the other hand, is not greatly affected when $\nabla[E]_{th}$ is increased because it results in a somewhat proportional decrease in number of both collected tumor cells and collected macrophages. However, increasing $\nabla[C]_{th}$ can eliminate the number of collected macrophages but the tumor cells still chemotact along the EGF gradient from the needle, therefore $\nabla[C]_{th}$ did not greatly affect the number of collected tumor cells. The ratio between collected tumor cells and macrophages changed when $\nabla[C]_{th}$ was increased because the number of collected macrophages decreased to zero while the number of collected tumor cells only decreased slightly.

These results can be compared to the *in vivo* experimental results from Wyckoff *et al.* [22]. The experiments were repeated with a cancer cell line that over-expressed the EGF receptor. The increase in EGF receptors resulted in a 70-100% increase in the number of tumor cells collected. If the increase in EGF receptors makes the cells more sensitive to EGF gradients, these results could be compared to the results in Figure 5.9.B. In the simulations, if the EGF gradient threshold was decreased from 0.2 to 0.02 nM the number of collected tumor cells increased from 28 to 46, which corresponds to about 65% increase. The increase in EGF receptors on the mutant cell line might also affect the secretion of CSF-1 by the tumor cells. Therefore, I also repeated the simulations making the cells secrete ten times more CSF-1. The simulations showed that the number of collected tumor cells increased from 28 to 53 which corresponds to a 90% increase. The simulation results seem to be in good agreement with the experimental results.

5.6 Concentration of EGF in the needle

I changed the concentration of EGF in the needle and investigated the effect it had on collected cells. Increasing the concentration of EGF in the needle increased the number of both collected tumor cells and macrophages (Figure 5.10). For low concentration of EGF in the needle (less than 5 nM), only a few tumor cells chemotacted into the needle because of sub-threshold gradient of EGF. When the EGF concentration in the needle was increased the gradient became steeper and thus more tumor cells migrated into the needle. The collected tumor cells secreted CSF-1 and

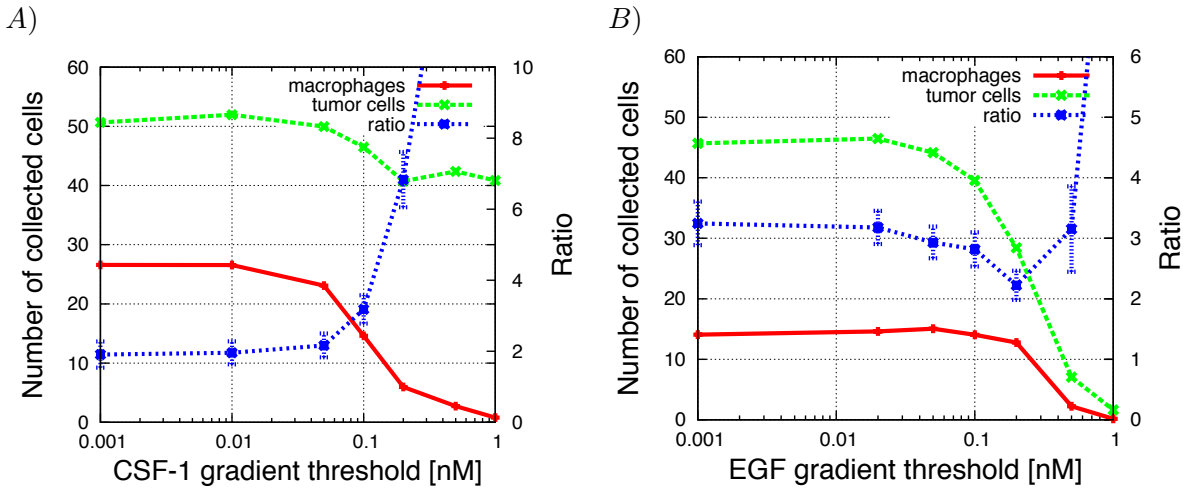

Figure 5.9: The number of collected tumor cells and macrophages as well as the ratio of collected tumor cells to macrophages (left y-axis) as a function of: A) CSF-1 gradient threshold for macrophages is increased, with $\nabla[E]_{th}$ = 0.02 nM. B) EGF gradient threshold for tumor cells, with $\nabla[C]_{th}$ = 0.1 nM.

when the number of collected tumor cells increased the CSF-1 gradient became steeper resulting in more macrophages being collected. The ratio of collected tumor cells to macrophages stayed fairly constant (between 2.5 to 3.5) when the concentration of EGF in the needle was increased. This was to be expected because increasing the concentration of EGF in the needle should not affect the number of macrophages that follow each tumor cell. The number of collected tumor cells and macrophages seemed to be increasing proportionally.

These simulation results can be compared to Figure 1.D. in Wyckoff [22] where they altered the concentration of EGF in the needle and demonstrated the effect it had on the total number of collected cells. In the experiments, the number of collected cells increased when the concentration of EGF in the needle was increased from 0–25 nM. In the simulations, the same trend is observed when increasing the concentration in the needle, thus the results from the simulations are in good agreement with the experimental results. However, when the concentration was increased to 50 nM in the experiments, the number of collected cells decreased. The simulation results did not show this decrease in number of collected cells. A possible explanation is that my model does not include the binding and unbinding of receptors. In the experiments, it is possible that nearly all the receptors were bound when the concentration in the needle was 50 nM and therefore a cell could not detect a

difference in bound receptors across its diameter. This hypothesis could be tested by including the binding and unbinding of receptors in the model. Another explanation may be that a non-monotonic response of the cells to EGF is needed. This may be due to internal signaling pathways that are not included in my model but could be added to investigate this hypothesis.

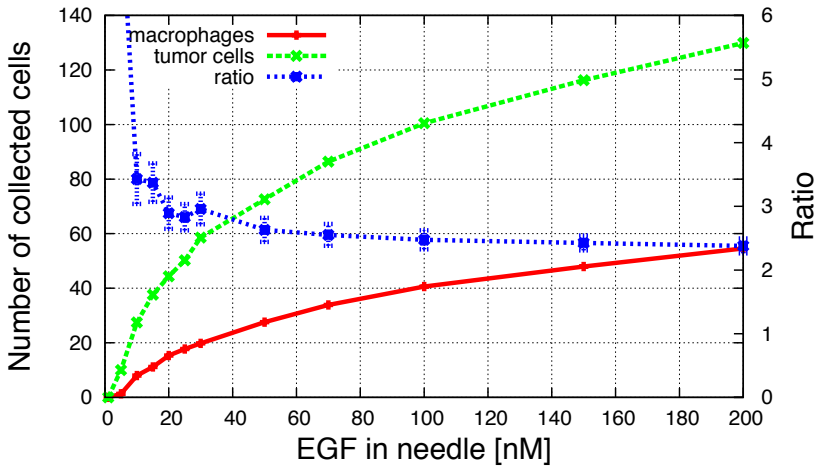

Figure 5.10: Number of collected tumor cells and macrophages as well as the ratio of collected tumor cells to macrophages as a function of the concentration of EGF in the needle. All other parameter values in Table 5.1 were kept constant.

5.7 Ratio of macrophages to tumor cells

At different locations within a tumor and in different patients the ratio between macrophages and tumor cells at the tumor margin varies. In this section, I explored how changing this initial ratio affected the number and ratio of collected cells. I refer to the percentage of macrophages of the total cells in the initial culture as the percentage of simulation macrophages.

When the percentage of simulation macrophages was increased the percentage of collected tumor cells decreased from 12 to 10% (Figure 5.11.B). The decreased density of tumor cells results in fewer tumor cells being close enough to the needle to detect a gradient of EGF above threshold. The number of collected tumor cells therefore decreased (Figure 5.11.A) even though the percentage of collected tumor cells did not change much. More interestingly, there was a biphasic curve for the number of collected macrophages when the percentage of simulation macrophages was increased.

The initial increase in collected macrophages was to be expected because increasing the percentage of simulation macrophages resulted in a higher density of macrophages. For more macrophages the CSF-1 gradient from the tumor cells was above threshold. When more than 50% of the total cells were macrophages the number of collected macrophages started decreasing, which, at first glance, was a more surprising result. This stems from fewer collected tumor cells and thus a sub-threshold gradient of CSF-1 for some of the macrophages.

When the percentage of simulation macrophages was increased the ratio of collected tumor cells to macrophages decreased until it reached a minimum of 1.4 when 70% of the total cells were macrophages (Figure 5.11.A). The decrease in ratio was caused by more macrophages following the tumor cells into the needle when the density of macrophages increased. Further increasing the percentage of simulation macrophages did not alter the ratio since at this point the collection of macrophages decreased linearly with the decrease in number of collected tumor cells.

These simulation results can be compared to experimental results from Wyckoff *et al.* [22] where a mutant cell line was used that had a lower density of macrophages around the tumor. In these experiments, the number of collected cells decreased by $\sim$80% compared to the wild-type and only 5–7% of collected cells were macrophages. In the simulation results in Figure 5.11.A, the number of collected tumor cells increased with decreasing percentage of simulation macrophages. Therefore, decreasing the percentage of macrophages at the tumor margin, while keeping all other parameters as before, does not compare to the simulation results with this mutant cell line. CSF-1 is known to recruit macrophages to the tumor sites. The mutant cell line in the experiment was defective in CSF-1 production. Therefore, I repeated the simulations with 10% macrophages in the initial culture as well as a decrease in CSF-1 secretion by the tumor cells. In simulations with 10% macrophages and k_{sec}^{tumor} = 0.002 nM/min only 10 tumor cells were collected on average and 0.2 macrophages compared to 45 tumor cells and 15 macrophages for simulations with 40% simulation macrophages and CSF-1 secretion coefficient of 0.02 nM/min. This corresponds to a 80% decrease in the number of collected tumor cells and only 2% of collected cells were macrophages. These simulation results seem to be in good agreement with experimental results.

5.8 Percentage of motile cells

Giampieri *et al.* [29] showed that the number of motile cells in mammary tumors can vary between 0–40%. I therefore repeated the simulations for different percentage of motile cells.

Increasing the percentage of motile cells increased the number of collected tumor cells and

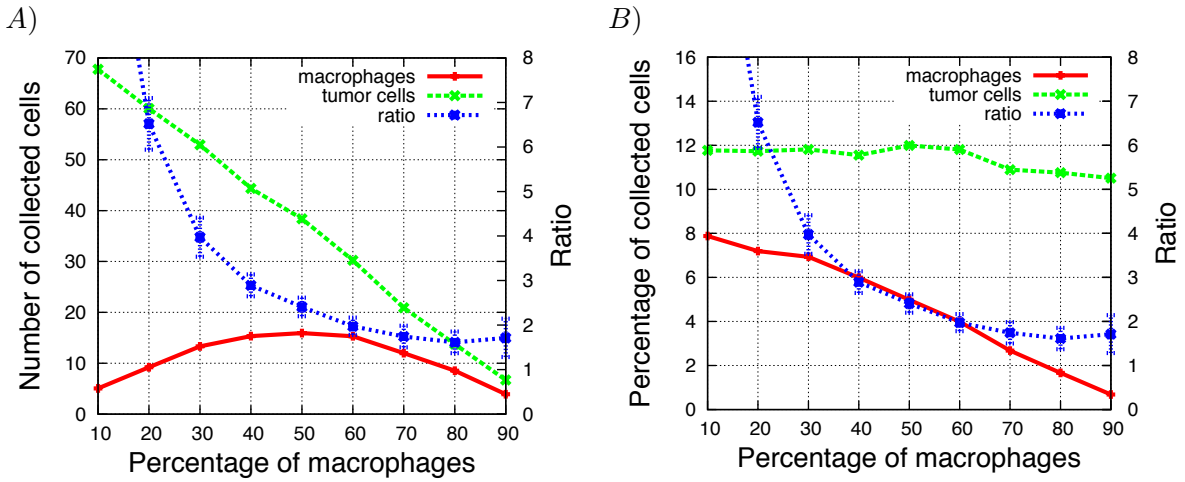

Figure 5.11: A) Number of collected tumor cells and macrophages as well as the ratio of collected tumor cells to macrophages as a function of percentage of simulation macrophages. B) Percentage of collected tumor cells and macrophages as a function of percentage of simulation macrophages. All parameter values from Table 5.1 were used.

macrophages. These results were to be expected because increasing the percentage of motile cells in the simulations caused more motile cells to be in the vicinity of the needle and therefore more cells chemotact into the needle. However, the ratio of collected tumor cells to macrophages decreased with increasing percentage of motile cells which was a more surprising result. The simulations were conducted using 1600 tightly packed cells. Increasing the percentage of motile cells did not increase the number of cells in the simulations but it made a higher percentage of the 1600 cells motile. The decreasing ratio between collected tumor cells and macrophages with increasing percentage of motile cells was likely caused by decreasing average distance between motile cells. For every tumor cell that chemotacted along the EGF gradient from the needle there were more macrophages in the tumor cell's vicinity that could migrate along the CSF-1 gradient from the tumor cell. Therefore, more macrophages could follow each tumor cell, which resulted in a decrease in the ratio of collected tumor cells to macrophages.

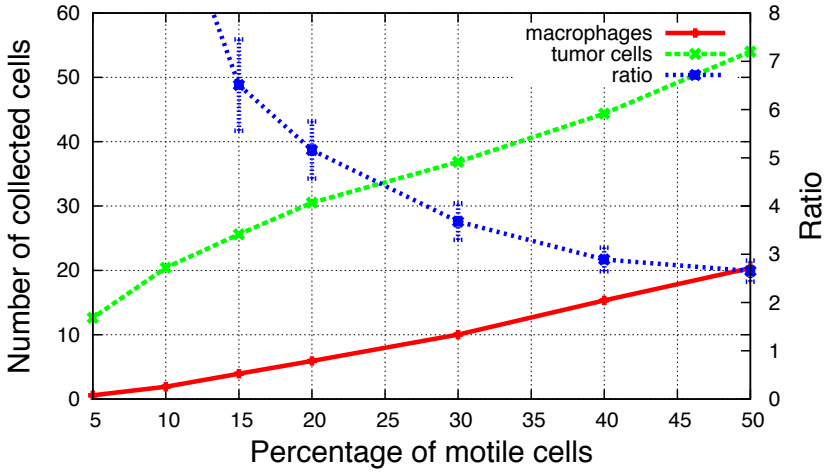

Figure 5.12: The number of collected tumor cells and macrophages as well as the ratio of collected tumor cells to macrophages as a function of percentage of motile cells. All other parameter values from Table 5.1 were kept constant.

5.9 Collection needle containing CSF-1

I repeated all of the simulations from the previous section with the same parameters except that the needle contained CSF-1 instead of EGF. As was to be expected, the results were symmetrical to the results from simulations with EGF in the needle. The collection of tumor cells now followed a similar trend as the collected macrophages did when the needle contained EGF and the collected macrophages followed a similar trend as the collected tumor cells did when the needle contained EGF. The ratio of collected tumor cells to macrophages was greatly affected when changing the concentration in the needle from EGF to CSF-1. In all of the simulations, more macrophages were now collected than tumor cells. Therefore, the ratio of tumor cells to macrophages was always less than 1. I will not display all of the results from these simulations here. Instead, I will compare the results when the needle contained CSF-1 and the CSF-1 membrane-bound degradation coefficient was changed to the results when the needle contained EGF and the EGF membrane-bound degradation coefficient was changed.

In Figure 5.13.A the needle contained EGF and in Figure 5.13.B the needle contained CSF-1. The number of collected tumor cells in Figure A has the same biphasic trend as the number of collected macrophages in Figure B. Similarly, the number of collected macrophages in Figure B can be

compared to the number of collected tumor cells in Figure B, and they also have comparable biphasic trends. The initial increase in collected cells was caused by the membrane-bound degradation making the gradient from the needle sharper, i.e. decreasing chemotaxis failure. The decrease in collected cells was caused by sub-threshold gradients of both EGF and CSF-1 when the membrane-bound degradation was increased. Because the two lines for tumor cells and macrophages switched, the ratios in the two graphs had opposite trends. In Figure 5.13.A the ratio increased with increasing EGF membrane-bound degradation and in Figure 5.13.B the ratio decreased with increasing CSF-1 membrane-bound degradation but in both cases there was paracrine enhancement.

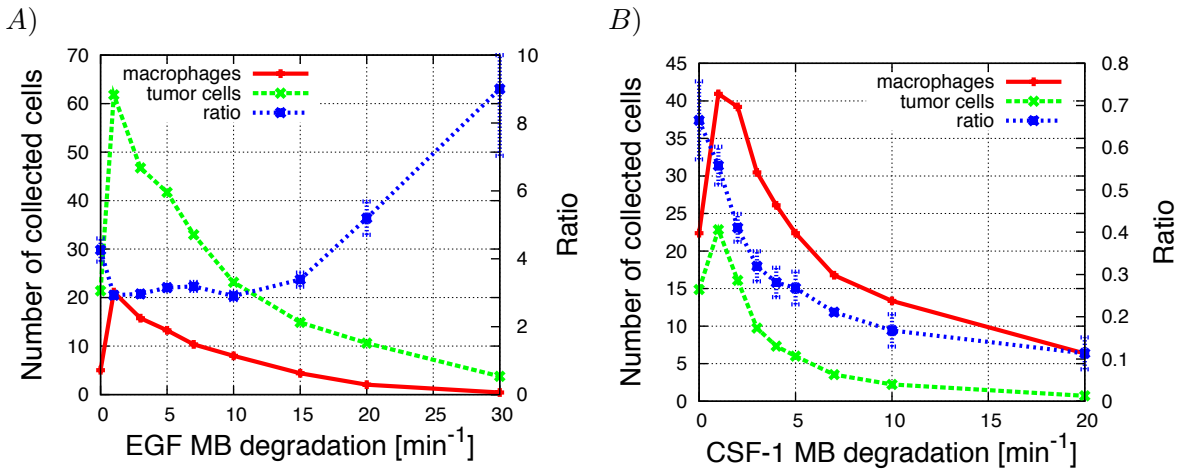

Figure 5.13: A) The number of collected tumor cells and macrophages as well as the change in the ratio of collected tumor cells to macrophages as a function of EGF membrane-bound degradation coefficient. The needle contains EGF and k_{mem}^{csf} = 1 min^{-1}. B) The number of collected tumor cells and macrophages when the CSF-1 membrane-bound degradation coefficient is increased as well as the change in the ratio of collected tumor cells to macrophages. The needle contains CSF-1 and k_{mem}^{egf} = 1 min^{-1}.

5.10 Generating a desired ratio with the needle containing CSF-1

In the simulations where the needle contained CSF-1 instead of EGF the ratio of collected cells was no longer close to 3 tumor cells to 1 macrophage. This is not altogether surprising. No results for the ratio between collected cells are reported in Wyckoff *et al.* [22]. The set of simulation parameters could be adjusted to produce the observed ratio of 3 tumor cells to 1 macrophage (Figure 5.14). This

required a fifteen fold greater CSF-1 degradation than EGF degradation and sevenfold greater EGF secretion than CSF-1 secretion. All parameter values as in Table 5.2.

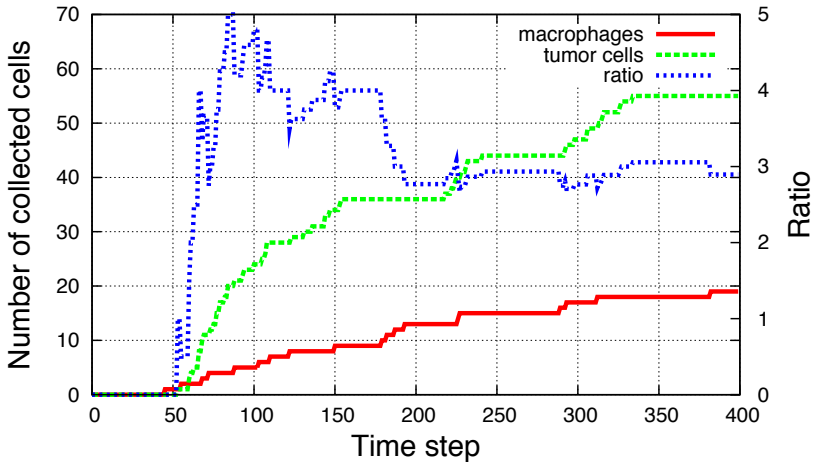

Figure 5.14: Changing the value of the membrane-bound degradation and secretion coefficients to get a ratio of 3 tumor cells to 1 macrophage when the needle contained CSF-1. Each time step corresponds to 5min. Values for all parameters in Table 5.2 were used in this simulation.

5.10.1 Membrane-bound degradation

Using the new parameter set given in Table 5.2, I investigated how changing the membrane-bound degradation of both EGF and CSF-1 altered the number of collected cells as well as the ratio of collected tumor cells to macrophages.

Increasing the CSF-1 membrane-bound degradation coefficient, with k_{mem}^{egf} = 1 min^{-1}, resulted in a biphasic curve for the number of collected tumor cells and macrophages (Figure 5.15.A). Initially, when k_{mem}^{csf} was increased that sharpened the CSF-1 gradient from the needle and decreased the chemotaxis failure by macrophages. Therefore, more macrophages were collected. The tumor cells followed the EGF gradient from the collected macrophages and therefore the number of collected tumor cells increased as well. For $k_{mem}^{csf} > 10$ min^{-1}, the number of collected macrophages decreased because for more macrophages there was a sub-threshold concentration of CSF-1. The number of collected tumor cells decreased because the decrease in collected macrophages caused a sub-threshold gradient of EGF from the, now fewer, collected macrophages. No cells were collected

Parameter	Value
External degradation*	0.02 min^{-1}
CSF-1 MB degradation*	15 min^{-1}
EGF MB degradation*	1 min^{-1}
CSF-1 secretion*	0.2 nM/min
EGF secretion*	0.03 nM/min
CSF-1 gradient threshold	0.1 nM
EGF gradient threshold	0.02 nM
CSF-1 in needle	20 nM
Percentage of macrophages	40%
Percentage of motile cells	40%

Table 5.2: **Parameter values** - List of parameters used to generate a desired ratio of 3 tumor cells to 1 macrophage when the needle contained CSF-1. MB: membrane-bound. *Note: these parameter values have been selected to fit this model, they should not be directly compared to parameters in other models or in experiments.

when $k_{mem}^{csf} > 30$ min^{-1}. The ratio of collected tumor cells to macrophages increased with increasing CSF-1 membrane-bound degradation coefficient up to a maximum value of 3, where it began to decrease.

Increasing the EGF membrane-bound degradation coefficient, with k_{mem}^{csf} = 15 min^{-1}, resulted in an initial increase in the number of collected tumor cells and macrophages. Further increasing the EGF membrane-bound degradation coefficient resulted in a decrease in the number of collected tumor cells and macrophages (Figure 5.15.B). The initial increase in the number of collected cells could be explained by the fact that when no EGF was degraded at the cell membranes there was a build up of EGF at the tumor margin. The build up of EGF resulted in fewer tumor cells chemotacting towards the collected macrophages and more CSF-1 being secreted at the tumor margin. When the EGF membrane-bound degradation was increased the gradient from the migrating macrophages became sharper and more tumor cells could follow the macrophages into the collection needle. The number of collected macrophages increased as well because of the paracrine enhancement. Further increasing the EGF membrane-bound degradation decreased the number of collected tumor cells because of a sub-threshold gradient or a sub-threshold concentration of EGF for more tumor cells. The number of collected macrophages only decreased slightly from the lack of paracrine enhancement. The EGF membrane bound degradation has a greater effect on the number of collected tumor cells than the number of collected macrophages, this causes the ratio of collected tumor cells to macrophages to follow the same biphasic trend as the number of collected tumor cells.

These results had similar progression as the results in Figure 5.4 where the needle contained

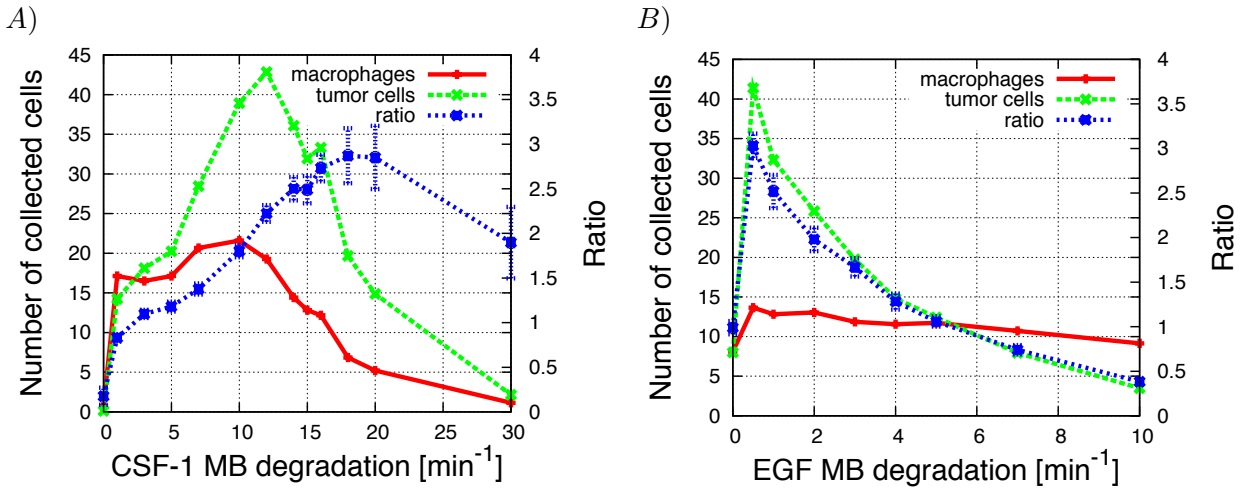

Figure 5.15: The needle contained CSF-1. A) The number of collected tumor cells and macrophages and the ratio between collected tumor cells and macrophages as a function of CSF-1 membrane-bound degradation coefficient, with k_{mem}^{egf} = 1 min^{-1}. B) The same quantities but for changes in the EGF membrane-bound degradation coefficient, with k_{mem}^{csf} = 15 min^{-1}.

EGF. Here, we should be comparing the collected macrophages in the simulations with EGF in the needle to the collected tumor cells in the simulations with CSF-1 in the needle, and vice versa. The same could be said about the trends in Figure 5.4.A and Figure 5.15.B.

5.10.2 Secretion coefficients

In the simulations with CSF-1 in the needle, the EGF secretion coefficient by macrophages was tenfold greater than for the simulations with EGF in the needle. In this section, I explored how changing both the EGF and CSF-1 secretion coefficients affected the number of collected cells.

Increasing the CSF-1 secretion coefficient for tumor cells, with k_{sec}^{macro} = 0.2 nM/min, resulted in a decrease in the number of tumor cells collected (Figure 5.16.A). The increase in k_{sec}^{tumor} activated non-invasive macrophages located at the tumor margin to secrete EGF, which resulted in chemotaxis failure for some tumor cells. The number of macrophages collected increased slightly to a maximum when k_{sec}^{tumor} = 0.05 nM/min. The higher secretion of CSF-1 by tumor cells resulted in more invasive tumor cells being able to recruit nearby macrophages to migrate into the needle as well. This is another example of paracrine enhancement and resulted in increased number of invasive macrophages. For $k_{sec}^{tumor} > 0.05$ nM/min the number of collected macrophages began to decrease

because of chemotaxis failure. When $k_{sec}^{tumor} > 1$ nM/min the chemotaxis failure by macrophages resulted in no cells being collected.

The ratio of collected tumor cells to macrophages decreased with increasing CSF-1 secretion coefficient which was to be expected since the tumor cells secreted CSF-1 and the macrophages chemotact towards CSF-1. Increasing the CSF-1 secretion coefficient results in decreasing number of collected tumor cells while the number of collected macrophages does not start decreasing until later and then at a slower rate. This results in the ratio between collected tumor cells and macrophages following the same decreasing trend as the number of collected tumor cells.

Increasing the EGF secretion coefficient, with k_{sec}^{tumor} = 0.03 nM/min, resulted in a maximum value for both collected macrophages and tumor cells but they had different inflection points (Figure 5.16.B). The number of collected tumor cells increased when the EGF secretion coefficient was increased because the EGF gradient was above threshold value for more tumor cells. When $k_{sec}^{macro} >$ 0.2 nM/min the number of collected tumor cells began to decrease. This was caused by chemotaxis failure by tumor cells. The number of collected macrophages increased slightly when the EGF secretion coefficient was increased until it reached a maximum. This stems from the paracrine enhancement. When the number of collected tumor cells decreased the number of collected macrophages decreased as well because of a decrease in paracrine enhancement.

The ratio of collected tumor cells to macrophages followed the same trend as the number of collected tumor cells. The tumor cells were more affected by changes in the EGF secretion coefficient than the macrophages. More tumor cells followed the macrophages into the needle when the EGF secretion coefficient was increased, which caused the ratio to increase.

Similarly to the previous section, these results had the same trends for number of collected cells as the results in Figure 5.6 where the needle contained EGF and the secretion coefficients were changed. The collected macrophages in the simulations with EGF in the needle could be compared to the collected tumor cells in the simulations with CSF-1 in the needle, and vice versa. Figure 5.6.A and Figure 5.16.B had the same trends and Figure 5.6.B and Figure 5.16.A had the same trends. Although the simulations with EGF and CSF-1 in the needle were conducted with different parameters, changing the degradation coefficients or secretion coefficients had a comparable effect on the collected tumor cells and macrophages.

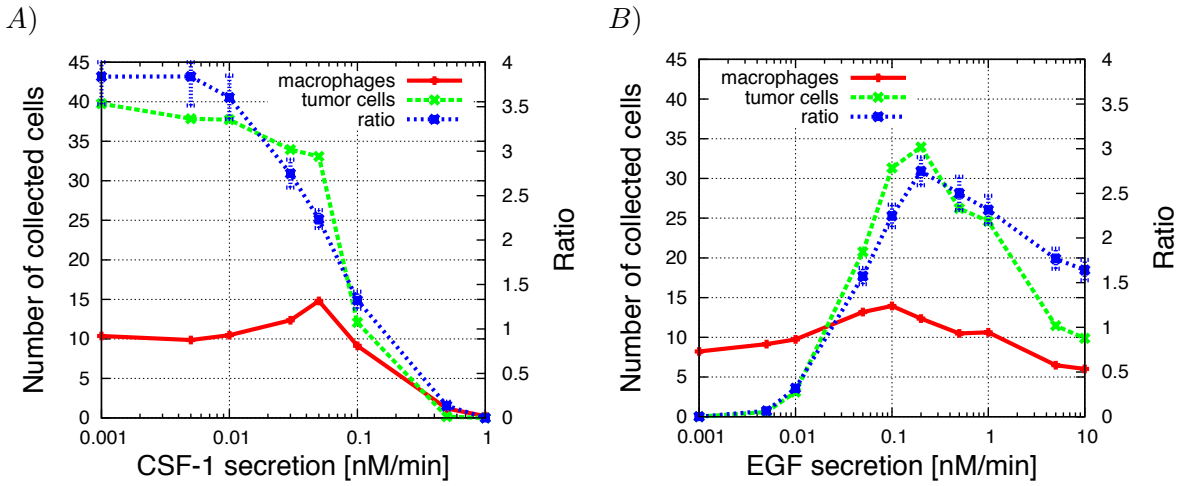

Figure 5.16: A) The ratio between collected tumor cells and macrophages as well as the number of collected tumor cells and macrophages as a function of CSF-1 secretion coefficient for tumor cells. k_{sec}^{macro} = 0.2 nM/min and the needle contains CSF-1. B) The ratio between collected tumor cells and macrophages as well as the number of collected tumor cells and macrophages as a function of EGF secretion coefficient by macrophages, with k_{sec}^{tumor} = 0.03 nM/min.

Chapter 6

Conclusions

I used my model to simulate the paracrine signaling between tumor cells and macrophages. Details regarding the internal biochemistry or mechanics of tumor cells and macrophages were not included. Instead the model simulated the response of the cells to an external stimulus. When a cell detected a signal and a gradient of either EGF (tumor cells) or CSF-1 (macrophages) it could chemotact along the gradient and start secreting CSF-1 (tumor cells) or EGF (macrophages). This simplified version of the system was sufficient to reproduce results from both *in vitro* and *in vivo* experiments. Simulations showed how certain parameters could eliminate the invasion of tumor cells. The model can, enhance our current understanding of the paracrine signaling loop and, be used to predict outcomes for changes in parameters and suggest experiments to verify those predictions.

6.1 Simulations of *in vitro* experimental setup

Simulation results, of the *in vitro* experimental setup in Goswami [21], showed that the number of invasive tumor cells could be altered by changing certain model parameters. Using the set of parameters listed in Table 4.1, I reproduced the experimental results of 25% invasive tumor cells all in close proximity to macrophages.

To gain confidence in the model more experiments need to be conducted to validate the simulation results. If experiments are not in agreement with the simulation results that will suggest that: (i) the EGF/CSF-1 paracrine signaling loop is not sufficient to explain the tumor cell invasion but that some other mechanism is necessary or (ii) the simplified version of the signaling pathway simulated here can not account for the behaviour of the two cell types. For (i) there could be another signaling molecule involved in the process or the interactions of the cells with the extracellular matrix might

Parameter	**How to eliminate invasive tumor cells**
CSF-1 MB degradation	Increase
EGF MB degradation	Increase
CSF-1 secretion	Does not occur
EGF secretion	Decrease
External CSF-1	Decrease
CSF-1 gradient threshold	Does not occur
EGF gradient threshold	Does not occur
Ratio of macrophages	Does not occur

Table 6.1: **Summary of *in vitro* simulations** - This table lists the parameters that were varied in the simulations. The second column shows which parameters could be altered by one order of magnitude or less to eliminate invasive tumor cells.

play a role. When EGF and CSF-1 receptors are bound it activates a cascade of internal signaling pathways. For (ii) including more of the cells internal response to an external stimuli might be necessary. The secretion of signaling molecules might need to be non-uniform. Modelling the binding and unbinding of receptors and the distribution of receptors on the cell membrane might also be a necessary enhancement to the model. In the next chapter, I suggest a few enhancements that can be made to the model.

In chapter 4, I conducted a parametric sensitivity analysis for the simulations of the *in vitro* experimental setup. The analysis showed how changing one parameter while keeping others constant affected the number of invasive cells. In Table 6.1, I have summarized which of these parameters could eliminate invasive tumor cells, if altered by one order of magnitude or less. This is of great importance because these parameters are potential targets in cancer chemotherapy.

The results from simulations in chapter 4 can be compared to two different experimental results from Goswami *et al.* [21]. In the experiments with MTLn3 tumor cells, 25% of the tumor cells were invasive but for MDA-MB-231 tumor cells 70% of the tumor cells were invasive. The results from the simulations suggest two possible reasons for the different level of invasiveness of the two cell types: (1) MDA-MB-231 cells have a higher membrane-bound degradation of CSF-1 than MTLn3 cell or (2) MDA-MB-231 cells secrete more CSF-1 than MTLn3 cells. The two different cell lines may vary in a number of ways and a combination of (1) and (2) could be taking place. This could be tested experimentally by, for example, measuring the local concentration of CSF-1.

The simulation results can also be compared to experimental results when MTLn3 cells were plated with LR5 macrophages or BAC macrophages. The experiments showed that the percentage

of invasive tumor cells was $\sim$25% in the presence of BAC macrophages but $\sim$15% when plated with LR5 macrophages. This can be compared to simulation results in Figure 4.7.B where increasing the EGF secretion coefficient by one order of magnitude altered the number of invasive tumor cells from $\sim$12% to $\sim$22%. Based on these results, one possibility is that LR5 macrophages secrete lower amounts of EGF than BAC macrophages.

The simulation results in Figure 4.8 can be compared to experimental results with Mena11a and Mena^{INV} cells. In simulations, increasing the EGF gradient threshold decreased the number of invasive tumor cells. Mena^{INV} cells are known to have a lower EGF gradient threshold value than the less invasive Mena11a cells. Simulation results are thus in good agreement with results from experiments with different Mena isoforms.

6.1.1 Future experiments for validation

Based on results from all these different simulations, I would suggest the following experiments to be conducted to validate the model:

- Use time-lapse imaging to view the motility of both tumor cells and macrophages in the Goswami *et al.* [21] experimental setup. The imaging would give more information about the motility patterns and the proximity of the two cell types. In the simulations, the macrophages seemed to move first in the direction of the CSF-1 gradient from the overlaid media and then the tumor cells followed them (Figure 4.3). The two cell types often moved in pairs.

- Repeat the experiments of Goswami *et al.* [21] with a different ratio between tumor cells and macrophages in the initial culture and look for changes in the number of invasive tumor cells. According to my model changing the percentage of macrophages in the initial culture changes the number of invasive cells. When less than 50% macrophages were in the initial culture more invasive tumor cells than macrophages were obtained. For an initial percentage of macrophages above 50% there were more invasive macrophages than tumor cells.

- Repeat the experiments of Goswami *et al.* [21] with different CSF-1 concentration in the media. The simulations showed an increase in number of invasive tumor cells and macrophages when the concentration of CSF-1 in the media was increased. It would also be of interest to repeat that experiment with EGF in the media instead of CSF-1.

- Repeat the experiments of Goswami *et al.* [21] with a mutant cell line(s) with a higher rate of degradation of the signaling molecules. In the simulations, the percentage of invasive

tumor cells were eliminated by changing the membrane-bound degradation coefficient by less than one order of magnitude. There was a maximum in the number of collected tumor cells and macrophages when the CSF-1 degradation was increased in simulations. When the EGF degradation was increased, there was a maximum in the number of collected tumor cells and the number of collected macrophages increased (Figures 4.6.A and B).

- Repeat the mRNA experiments of Goswami *et al.* [21] and report the precise readings for concentration of EGF and CSF-1. The mRNA levels could be used to estimate the secretion coefficients in my model.

- Repeat the experiments by Goswami *et al.* [21] with different doses of receptor blockers. Results from that experiment could be compared to the simulation results. The receptor blockers are likely changing multiple functions of cells. For example, blocking EGF receptors might make cells less sensitive to gradients of EGF and it might also cause them to secrete less CSF-1. This would need to be considered when comparing the experimental results to the simulation results.

6.2 Simulations of the *in vivo* experimental setup

My simulations reproduced the experimental results of 3 tumor cells per 1 macrophage migrating into collection needles. This was achieved by using the same parameters I used for simulating the *in vitro* experimental setup, (Table 5.1) and changing the setup to fit the *in vivo* experimental setup from [22]. However, not surprisingly that same set of parameters did not reproduce the same ratio when the collection needle contained CSF-1 instead of EGF. In Wyckoff *et al.* [22], no data about the ratio of the collected cells is given for the experiments, when the needle contained CSF-1 they just note that similar results are obtained as when the needle contained EGF. When the needle contains CSF-1 a different set of parameters was required to reproduce the ratio of 3 tumor cells per 1 macrophage migrating into the collection needle. More experiments and simulations are needed to explain the difference in the ratio between collected cells. A good first step would be to parametrize the model with experiments.

The 3 to 1 ratio between the collected tumor cells and macrophages could be altered by changing many of the model parameters. However, it was more sensitive to changes in some parameters than others, Table 6.2. It was most sensitive to changes in the CSF-1 membrane-bound degradation coefficient, the percentage of macrophages in the simulation and the percentage of motile cells.

Ratio less sensitive to changes in:	Ratio more sensitive to changes in:
EGF MB degradation	CSF-1 MB degradation
EGF secretion	Percentage of macrophages
CSF-1 secretion	Percentage of motile cells
EGF gradient threshold	
CSF-1 gradient threshold	
EGF in needle	
External degradation of EGF and CSF-1	

Table 6.2: **Sensitivity of the ratio to changes in parameters** - This table summarizes the sensitivity of the ratio between collected tumor cells and macrophages to model parameters. Note that all of the model parameters affect the ratio but not to the same extent.

Parameter	How to eliminate invasive tumor cells
External degradation of EGF and CSF-1	Increase
CSF-1 MB degradation	Does not occur
EGF MB degradation	Increase
CSF-1 secretion	Does not occur
EGF secretion	Increase
EGF in needle	Decrease
CSF-1 gradient threshold	Does not occur
EGF gradient threshold	Increase
Percentage of macrophages	Does not occur
Percentage of motile cells	Does not occur

Table 6.3: **Summary of *in vivo* simulation results** - This table lists the parameters that were varied in the simulations. The invasiveness of tumor cells was more sensitive to changes in some parameters than others. The second column shows which parameters could be altered by one order of magnitude or less to eliminate invasive tumor cells.

It was less sensitive to changes in the EGF membrane-bound degradation coefficient, the external degradation coefficient, the secretion coefficients, the gradient thresholds and the amount of EGF in the needle.

In Table 6.3, I have summarized the results from a parametric sensitivity analysis of simulations with the needle containing EGF to identify which parameters could be altered by less than one order of magnitude to eliminate the number of tumor cells collected. Identifying these parameters is important when searching for new targets in chemotherapy.

I compared the results from simulations to experimental results with various alterations. In experiments, Wyckoff *et al.* [22] used a mutant cell line that over-expressed the EGF receptor. I

assumed that would make the tumor cells more sensitive to gradients of EGF and that it would increase the secretion of CSF-1. In the experiments with the mutant cell line , a 70–100% increase in collected tumor cells was reported. In the simulations there was a 65–90% increase in collected tumor cells. These results from simulations and experiments were in good agreement.

Simulation results can also be compared to experimental results with a mutant cell line defective in CSF-1 production and with a low density of macrophages at the tumor site. In experiments with this cell line, the number of collected cells decreased by $\sim$80% and only 5–7% of collected cells were macrophages. In the simulations, when 10% of cells were macrophages and the secretion of CSF-1 by tumor cells was decreased ten fold the number of collected cells decreased by 80% and only 2% of collected cells were macrophages, which was also in good agreement with experimental results.

6.2.1 Future experiments for validation

The simulations for the *in vivo* experimental setup need to be validated with experiments. This is not as straight forward as for the *in vitro* experiments where everything can be fairly easily controlled. The *in vivo* experiments are performed in live mice where the extracellular matrix can be difficult to manipulate and using a different cell line might alter more than just the cells response. Following are suggestions of experiments to be conducted to validate the simulation results:

- Repeat the experiments by Wyckoff *et al.* [22] with a mutant tumor cell line(s) and macrophage(s) that degrade more EGF. According to the simulation results, the number of collected tumor cells is sensitive to changes in the EGF membrane-bound degradation.

- Repeat the experiments by Wyckoff *et al.* [22] with a less motile cell line (or more Mena11a cells). Decreasing the percentage of motile cells resulted in a decrease in the number of tumor cells and macrophages collected in the simulations.

- Repeat the experiments by Wyckoff *et al.* [22] with increased density of macrophages at the tumor margin. Increasing the percentage of macrophages in the simulations resulted in a decrease in the number of collected tumor cells and a maximum number of collected macrophages.

- Repeat the experiments by Wyckoff *et al.* [22] with different doses of receptor blockers which can affect the gradient threshold values, the secretion coefficients and/or the degradation coefficients. Results from those experiment could be compared to a number of simulation results,

depending on what function of the cells the receptor blockers alter.

These are only a few suggestions for experiments that could be conducted to validate the models and is in no means a finite list. The important thing is to repeat experiments with different biological parameters that correspond to the parameters in the model and to compare the experimental results to the simulation results.

Cancer cells have been shown to develop resistance to the current drug therapies. Enhancing our understanding of the paracrine signaling between tumor cells and macrophages may help in identifying new targets in chemotherapy that are not likely to be affected by evolved drug resistance.

Chapter 7

Future enhancements

I have identified future enhancements that can be implemented into the model to continue research on motility of breast cancer cells once the current computational framework has been validated with experiments.

7.1 Receptor distribution

In Wyckoff *et al.* [22], the number of collected cells increased when the concentration of EGF in the needle was increased until it reached a maximum at 25 nM. When the concentration was increased to 50 nM, the number of collected cells decreased. This did not correlate with the simulation results where the number of collected cells increased with increasing concentration of EGF in the needle. A possible explanation for the decrease in collected cells in the experiment is that when the concentration in the needle was very high, all the EGF receptors on the tumor cells were bound and therefore the cell could not detect a difference in chemical concentration across its diameter. To capture this behaviour the receptors on the cells need to be added to the model. The number of bound receptors at the leading edge and at the rear-end would be compared to calculate the gradient. Incorporating the receptors in the model would require using coupled ordinary differential equations to describe the change in bound receptors over time.

It might also be of interest to study the effect that different distributions of receptors on the membrane, would have on the results. A higher density of receptors might be located at the leading edge, which can be easily examined with the model. Here, the ellipsoidal shape of the cells could be of importance. Adding this anisotropic receptor distribution might be crucial to get the distinct streaming pattern mentioned in Wyckoff *et al.* [6].

7.2 Autocrine loop

The current model simulates the paracrine signaling loop between tumor cells and macrophages which involves CSF-1 and EGF. Experiments by Patsialou *et al.* [30] have shown that in addition to the paracrine loop there is also a CSF-1/CSF-1R autocrine loop that is involved in the invasion of human breast cancer cells. These experiments were conducted using the human breast cancer line MDA-MB-231 in mice. The MDA-MB-231 cells have EGF receptors and secrete CSF-1 like the PyMT and MTLn3 cell lines used in Wyckoff *et al.* [22], but they also have CSF-1 receptors which enables autocrine signaling. These cancer cells can thus enhance the motility of other cancer cells. Results from both *in vivo* and *in vitro* experiments are reported in Patsialou *et al.* [30]. The *in vitro* experimental setup is the same as described in chapter 2.1, where the cells are plated on a MatTek dish, overlaid by collagen and media containing CSF-1 is placed on top of the collagen. The *in vivo* experimental setup is the same as described in chapter 2.2, where they use micro-needles containing either EGF or CSF-1 to collect cells that migrate towards the gradient from the needle.

In *in vitro* experiments [30] using MDA-MB-231 cells the number of invasive tumor cells increases greatly in the presence of macrophages which suggests that *in vitro* the paracrine loop is more effective in promoting invasion than the autocrine loop. Results from *in vivo* experiments [30] showed that invasion of this cell line is less dependent on the macrophages, where only 6% of the collected cells were macrophages (compared to 25% in the experiments with MTLn3 and PyMT cell lines simulated in this work). They also showed that the concentration of CSF-1R *in vivo* increases in the presence of TGFβ1.

It is possible and would be very interesting to include this CSF-1/CSF-1R autocrine loop in my model. This would involve an additional term in the PDE for CSF-1 concentration as well as changing the response of a tumor cell to also include CSF-1R binding. Results from these simulations could then be compared to the results in Patsialou *et al.* [30] .

7.3 Extracellular matrix

The extracellular matrix (ECM) refers to the microenvironment of a tumor and it greatly affects tumor progression. It is comprised of various molecules and growth factors as well as fibres, such as collagen. Fibronectin is also present in the ECM and it binds cells to collagen fibres. Collagen fibres can act as pathways for the cells to crawl along. In this model, the collagen fibres have not been modelled specifically. However, in the simulations the cells have been allowed to move

through the extracellular matrix assuming they are moving along collagen fibres. One way to model the extracellular matrix would be to use anisotropic diffusion of EGF and CSF-1. The idea is that the anisotropic diffusion could act as highways, making it easier for the cells to migrate in certain directions which would correspond to the collagen fibres. In these simulations the 3D capabilities of the model would be of great importance because a cell crawling along a collagen fibre might need to be able to move to another collagen fibre to move past other cells which is not possible in a 2D simulation. Another way to simulate the collagen fibres would be to make random tracks of EGF or CSF-1 which the cells could chemotact along.

7.4 Intravasation and extravasation

The focus of this research has been on how breast cancer cells can migrate from a primary tumor site and invade surrounding tissues or migrate towards blood vessels. When a tumor cell gets to a blood vessel it needs to squeeze through the wall of the blood vessel to get into the blood stream. Once they are in the blood stream they also need to be able to extravasate at distant sites to start forming secondary tumors. These intravasation and extravasation processes have not been included in this model thus far.

As mentioned earlier, macrophages associated with tumors are usually divided into two groups, TAMs and PMs. The TAMs are the ones that have been modelled here and enhance the motility of breast cancer cells. The PMs are believed to be involved in intravasation and extravasation. One step in improving the current model could be to include another cell type which would represent the PMs. According to Wyckoff *et al.* [6] these macrophages behave differently than the TAMs and they can exist as single cells or as clusters at the blood vessel sites. Because this is a force based model it can be used to simulate the mechanics in which a cell is capable of squeezing through the wall of the blood vessels. The deformability of the ellipsoids will also be an important feature in the model to simulate this movement through the wall of the blood vessels.

7.5 Other applications

In principle, this computational framework is not limited to breast cancer motility research but it can be applied to any biological system based on adhesiveness of cells and/or cell-cell signaling. Wound healing, epithelial-mesenchymal transitions (EMT), early zebrafish development, formation of new blood vessels and other types of cancer are a few examples of such biological systems.

Glioma (cancer initiated in the brain and in the spine) is one type of cancer where this model could be useful. Spreading of glioma has been shown to be greatly dependent on both paracrine signaling, between tumor cells and either TAMs, or microglia, and autocrine signaling (involving EGF and/or TGFα) [31]. Glioma is highly invasive and patients have a poor prognosis. Hence, it is both interesting and critical to enhance our current understanding of this disease. Some adjustments to the current computational framework would be necessary after which a parametric sensitivity analysis might yield new insights into the spreading of the cancer cells.

EMT is a process in which polarized cells in an epithelial layer lose their epithelial characteristics and become motile. EMT is an important process for early embryonic development but it is also responsible for increased invasiveness and metastatic potential of tumor cells. Our computational framework can be used to simulate this process. It involves adhesion of an epithelial cell to its neighbours and possibly a chemotactic signal of some sort that enables the cancerous cells to migrate away from the epithelial sheet.

Appendix A

Mathematical analysis in 1D

The computational model developed in this research has 3D capabilities which are important when studying the motility behaviour and the ratio between collected tumor cells and macrophages. Here, I will show results from a 1D mathematical analysis of a system that behaves similarly to the EGF/CSF-1 paracrine signaling between tumor cells and macrophages described in chapter 1. This work was conducted under the supervision of Dr. L. Edelstein-Keshet at the Department of Mathematical Biology at UBC. We wanted to know if behaviour in the more complicated 3D system could be explained analytically. Although the 1D system can not give as much insight into the motility of cells it can help explore the parameter space and identify conditions necessary for instability. I used a set of 4 PDEs to describe the system and performed linear stability analysis to find out if spontaneous aggregation of cells could occur and if so what conditions were necessary. The methods used for this analysis were adopted from work done by Luca *et al.* [32]. I also simulated the 1D system in Matlab and compared the numerical results to the mathematical analysis.

A.1 PDE system

The following set of PDEs are used to describe the signaling pathway between tumor cells and macrophages:

$$\frac{\partial \phi}{\partial t} = \mu \frac{\partial^2 \phi}{\partial x^2} - \frac{\partial}{\partial x}(\chi_1 \phi \frac{\partial c}{\partial x}) \tag{A.1}$$

$$\frac{\partial T}{\partial t} = \mu \frac{\partial^2 T}{\partial x^2} - \frac{\partial}{\partial x}(\chi_2 T \frac{\partial e}{\partial x}) \tag{A.2}$$

$$\frac{\partial c}{\partial t} = D\frac{\partial^2 c}{\partial x^2} + s_1 T - \gamma_1 c \quad (A.3)$$

$$\frac{\partial e}{\partial t} = D\frac{\partial^2 e}{\partial x^2} + s_2 \phi - \gamma_2 e \quad (A.4)$$

Where ϕ is the density of macrophages, T is the density of tumor cells, c is the CSF-1 concentration, e is the EGF concentration, μ is the random motion of cells, χ_i are the chemotaxis coefficients, D is the diffusion coefficient for the two signaling molecules, s_i are the secretion coefficients, γ_i are the degradation coefficients and $i \in \{1, 2\}$.

In this system the cells are free to move around randomly, the macrophages can chemotact towards a gradient of CSF-1 (second term in Equation A.1) and the tumor cells can chemotact towards a gradient of EGF (second term in Equation A.2). The two signaling molecules are free to diffuse around, CSF-1 is secreted by tumor cells (second term in Equation A.3) and degraded uniformly (third term in Equation A.3). EGF is secreted by macrophages (second term in Equation A.4) and degraded uniformly (third term in Equation A.4). There are two important differences between the system described by these equations and the ones used in the 3D model. Here,

- there is no membrane bound degradation but only external degradation.
- the secretion of signaling molecules has no upper or lower bound like the sigmoidal secretion in the 3D model and it does not depend on the concentration of the other signaling molecule around the cell. Instead, there is a linear relationship between the density of cells and the secretion of signaling molecules.

The system is assumed to have no flux boundary conditions. Therefore:

$$\mu\frac{\partial \phi}{\partial x} - \chi_1 \phi \frac{\partial c}{\partial x} = 0, \qquad \frac{\partial c}{\partial x}|_{0,L} = 0 \quad (A.5)$$

$$\mu\frac{\partial T}{\partial x} - \chi_2 T \frac{\partial e}{\partial x} = 0, \qquad \frac{\partial e}{\partial x}|_{0,L} = 0 \quad (A.6)$$

I used no flux boundary conditions because the *in vitro* experiments are conducted on a MatTek dish where there is no flux of material in and out of the dish.

If a well mixed system is assumed the diffusion terms go to zero. At the homogeneous steady state:

$$\tilde{T} s_1 = \gamma_1 \tilde{c} \Rightarrow \tilde{c} = \frac{\tilde{T} s_1}{\gamma_1} \quad (A.7)$$

$$\tilde{\phi} s_2 = \gamma_2 \tilde{e} \Rightarrow \tilde{e} = \frac{\tilde{\phi} s_2}{\gamma_2} \tag{A.8}$$

Here, $\tilde{X}$ is representative of the steady state concentration.

In order to simplify the PDE system and reduce the number of parameters, the equations can be written in a dimensionless form that results in the following equations:

$$\frac{\partial \phi}{\partial t} = \frac{\partial^2 \phi}{\partial x^2} - \frac{\partial}{\partial x}(A_1 \phi \frac{\partial c}{\partial x}) \tag{A.9}$$

$$\frac{\partial T}{\partial t} = \frac{\partial^2 T}{\partial x^2} - \frac{\partial}{\partial x}(A_2 T \frac{\partial e}{\partial x}) \tag{A.10}$$

$$\epsilon \frac{\partial c}{\partial t} = \frac{\partial^2 c}{\partial x^2} + a^2(T - c) \tag{A.11}$$

$$\epsilon \frac{\partial e}{\partial t} = \frac{\partial^2 e}{\partial x^2} + (\phi - e) \tag{A.12}$$

Where:

$$A_1 = \frac{\chi_1 \tilde{T} s_1}{\gamma_1 \mu}, \qquad \epsilon = \frac{\mu}{D} \tag{A.13}$$

$$A_2 = \frac{\chi_2 \tilde{\phi} s_2}{\gamma_2 \mu}, \qquad a^2 = \frac{\gamma_1}{\gamma_2} \tag{A.14}$$

By writing the equations in this dimensionless form the number of parameters reduces from 8 to 4.

A.2 Reduction to a system of 2 equations

To study this system analytically in more detail it is beneficial to first simplify it. A quasi steady state of c and e is assumed because the chemicals diffuse more rapidly than the random motion of the cells, meaning that $\mu << D$ and ϵ is small. Equations A.11 and A.12 then become:

$$0 = \frac{\partial^2 c}{\partial x^2} + a^2(T - c) \tag{A.15}$$

$$0 = \frac{\partial^2 e}{\partial x^2} + (\phi - e) \tag{A.16}$$

Green's functions can be used as solutions to these equations. Namely,

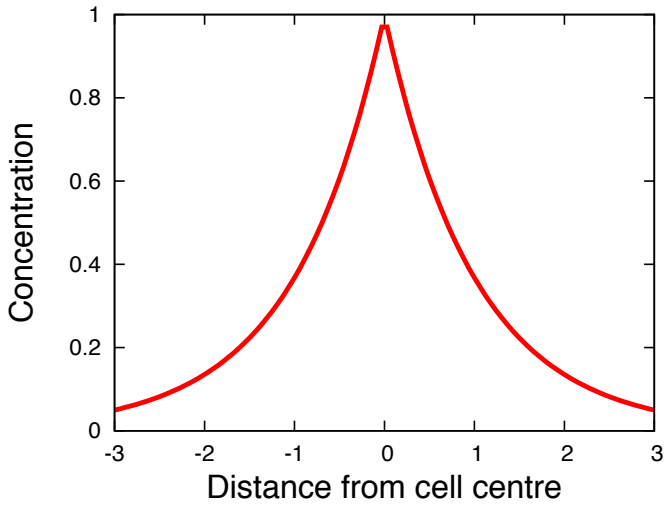

Figure A.1: In Equations A.17 and A.18 the concentrations of CSF-1 and EGF have been represented in terms of the position, x', of the tumor cells or macrophages. This graph represents the concentration profile from a cell located at x=0.

$$c = \frac{a}{2}\int_{-\infty}^{\infty} e^{-a|x-x'|}T(x')dx' \tag{A.17}$$

$$e = \frac{1}{2}\int_{-\infty}^{\infty} e^{-|x-x'|}\phi(x')dx' \tag{A.18}$$

The signaling molecule concentrations are now represented as functions that decrease exponentially with distance away from the cells, see Figure A.1. Concentration of EGF is represented with respect to the position of macrophages and concentration of CSF-1 is represented with respect to the position of tumor cells. Using these Green's functions for the concentration of e and c, the system can now be reduced to 2 PDEs containing convolution integral terms.

A.3 Linear Stability Analysis

By making some reasonable assumptions about the system the number of PDEs has been reduced from four to two. A linear stability analysis can be performed to see if a small perturbation from the steady state can cause spontaneous aggregation of the cells. The following perturbations are introduced in the system:

$$\begin{aligned} T &= \tilde{T} + T' e^{iqx+\sigma t} \\ \phi &= \tilde{\phi} + \phi' e^{iqx+\sigma t} \end{aligned} \tag{A.19}$$

Where q is the wavenumber of the perturbation and σ is the growth rate of the perturbation. Introducing this perturbation into the system and taking the relevant derivatives the following Jacobian is obtained:

$$J = \begin{bmatrix} \sigma + q^2 & -\frac{q^2 A_1 \tilde{\phi}}{q^2+a^2} \\ -\frac{q^2 A_2 \tilde{T}}{q^2+1} & \sigma + q^2 \end{bmatrix} \tag{A.20}$$

For non-trivial solutions the determinant of the Jacobian needs to be zero, $det(\mathbf{J}) = 0$. The eigenvalues of this Jacobian matrix will be of the form $\sigma^2 + B\sigma + C = 0$. Where:

$$B = 2q^2 \tag{A.21}$$

$$C = q^4(1 - \frac{A_1 A_2 \tilde{\phi}\tilde{T}}{(q^2+a^2)(q^2+1)}) \tag{A.22}$$

For spontaneous aggregation to occur, the small perturbations have to cause instability in the system. The growth rate, σ, needs to be positive to promote instability, which requires C<0. At the limit $q \to \infty$, C>0 and therefore instability can never occur for perturbations with large wavenumbers. Instability can occur if the following inequality is satisfied:

$$(q^2 + a^2)(q^2 + 1) < A_1 A_2 \tilde{\phi}\tilde{T} \tag{A.23}$$

This inequality gives insight into parameter regime where instability and thus spontaneous aggregation of cells can occur. For large enough values of A_1 and A_2 this inequality can be satisfied. Recall that $A_i \propto \frac{\chi_i s_i}{\gamma_i}$. In the limits where one of the secretion coefficients or one of the chemotaxis parameters goes to zero no spontaneous aggregation of cells can occur. The same holds true if one of the degradation coefficients is large.

A.4 Simulations

I used Matlab to simulate the set of 4 PDE system, equations A.1-A.4, for different values of A_i. I introduced a small perturbation in the concentration of T and the simulation results can be seen

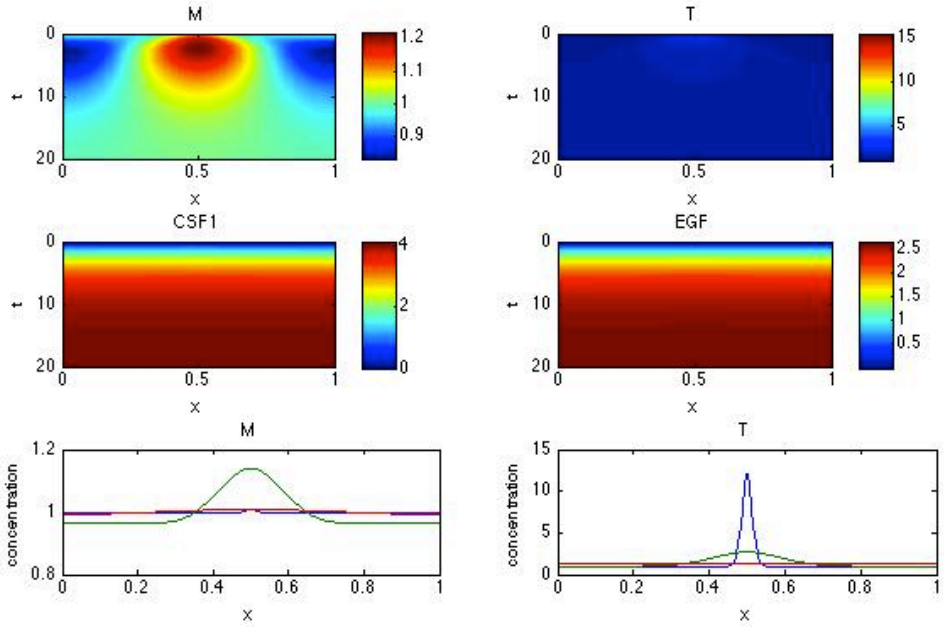

Figure A.2: A Gaussian peak perturbation in T is introduced in the centre of the simulation. In these simulations A_i is small and the system goes to equilibrium. M: macrophages, T: tumor cells. The first two rows are kymographs which show density of cells (first row) and concentration of signaling molecules (second row) with respect to position (x-axis) and time (y-axis). The third row shows the density of cells with respect to position for three different times in simulation, first blue, second green and third is red.

in Figures A.2-A.5. The figures are kymographs which show the concentration of tumor cells, macrophages, CSF-1 and EGF with respect to position (x-axis) and time (y-axis). If the A_i value is small than the small perturbation will die out and the system will equilibrate whereas if the A_i value is large there will be instability in the system and the two cell types aggregate around the position where the perturbation was introduced. These simulations validate the findings from the linear stability analysis in the previous section.

A.5 Conclusions

Carefully chosen assumptions about the diffusion rates and the homogeneous steady state help reduce the system of 4PDEs to a system of 2 PDEs. I studied the 2 PDE system analytically and arrived at the inequality in equation A.23. The 1D simulations in Matlab verify the findings from the linear

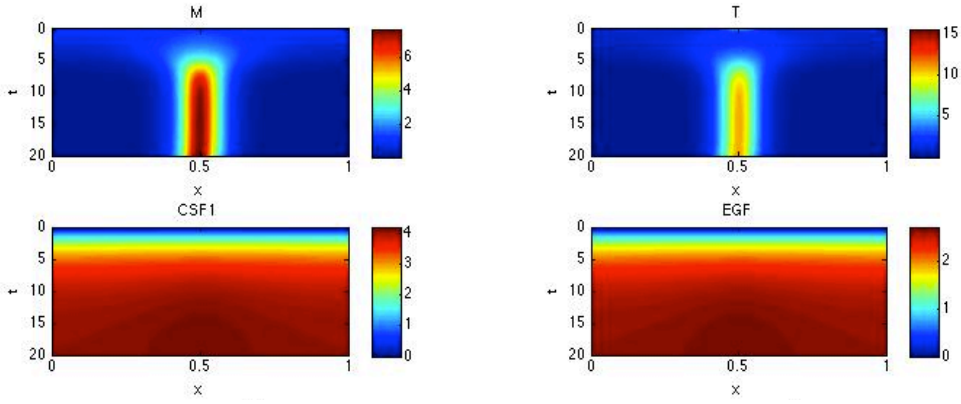

Figure A.3: As in Figure A.2 but for large A_i where instability occurs. The two cell types aggregate in the centre.

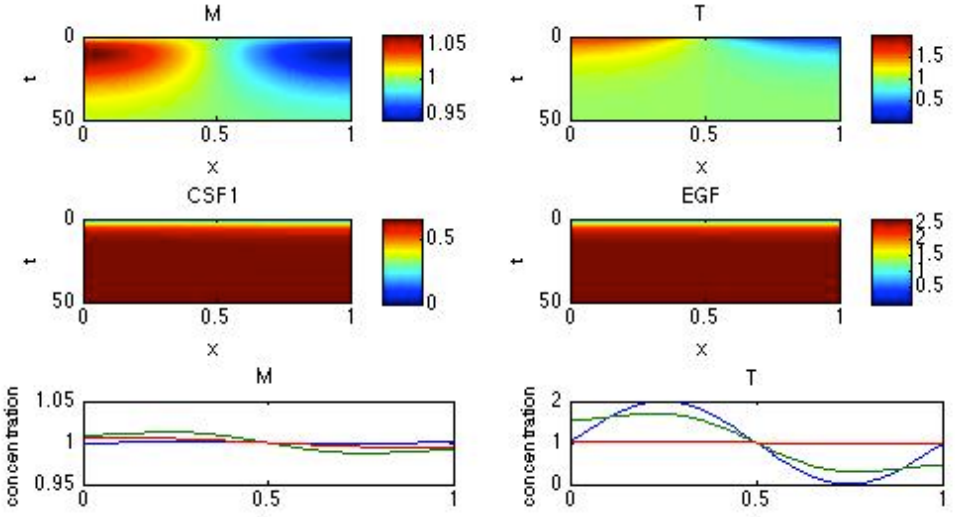

Figure A.4: A sine wave perturbation in T is introduced in the simulation. In these simulations A_i is small and therefore the system goes to equilibrium.

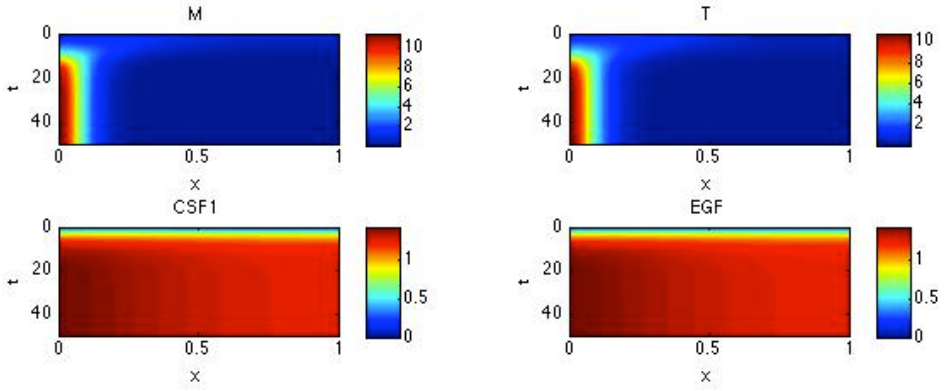

Figure A.5: As in Figure A.4 but for a large A_i causing instability and the two cell types aggregate on the left hand side.

perturbation analysis of the system. The results from these simulations can not be directly compared to the simulation results for the 3D model in chapters 4 and 5 because there are two important differences between the two systems. The 1D system does not have membrane bound degradation and the secretion is linear in the 1D system but sigmoidal in the 3D system. However, I conducted a couple of simulations with the 3D model that could be compared to these results. I randomly distributed the two cell types in the x-y plane and then I introduced a few active tumor cells in the centre of the x-y plane (Figure A.6). For low degradation coefficients the two cell types aggregate around the centre. For high degradation coefficients the two cell types are randomly distributed. The ratio between the two degradation coefficients is the same in both of the simulations, i.e. a^2 does not change. The 1D analysis therefore accurately predicts results from simulations with the 3D computational model.

The simplified secretion and degradation terms were chosen for this work in order to be able to analyze the system mathematically. The full system of 4 PDEs can be altered and studied in more detail numerically. The degradation and secretion terms can be changed to more closely resemble the 3D system and results can be compared to results from the 3D model. Future work with this 1D model may include: (a) making the secretion terms sigmoidal and dependent on the concentration of the other signaling molecule, (b) including membrane bound degradation. The size and ratio between cell types in the aggregates for different secretion and membrane-bound degradation coefficients can than be compared to the results from the 3D simulations.

The inequality in equation A.23 gives some useful insight into the parameters in the system. Increasing one of the secretion coefficients or decreasing one of the degradation coefficients can

result in instability and hence aggregation of cells. This is an important feature of the paracrine signaling loop where both signaling molecules are necessary for the two cell types to communicate. Another important result from the analysis is that if degradation of either signaling molecule is high that can result in discontinued interactions between the cell types and the system goes back to a homogenous steady state. The ratio between the two degradation coefficients is also important, through the parameter a^2 in equation A.11 and in the inequality in A.23. These results indicate that for instability to occur:

- both EGF and CSF-1 need to be present.
- increasing secretion of either of the signaling molecules is sufficient.
- the chemotaxis coefficients need to be large enough.

In conclusion, the paracrine signaling between tumor cells and macrophages is necessary for spontaneous cell aggregation. Altering the secretion coefficients, the degradation coefficients or the chemotaxis coefficients can disrupt the paracrine signaling and leave the cells immobilized.

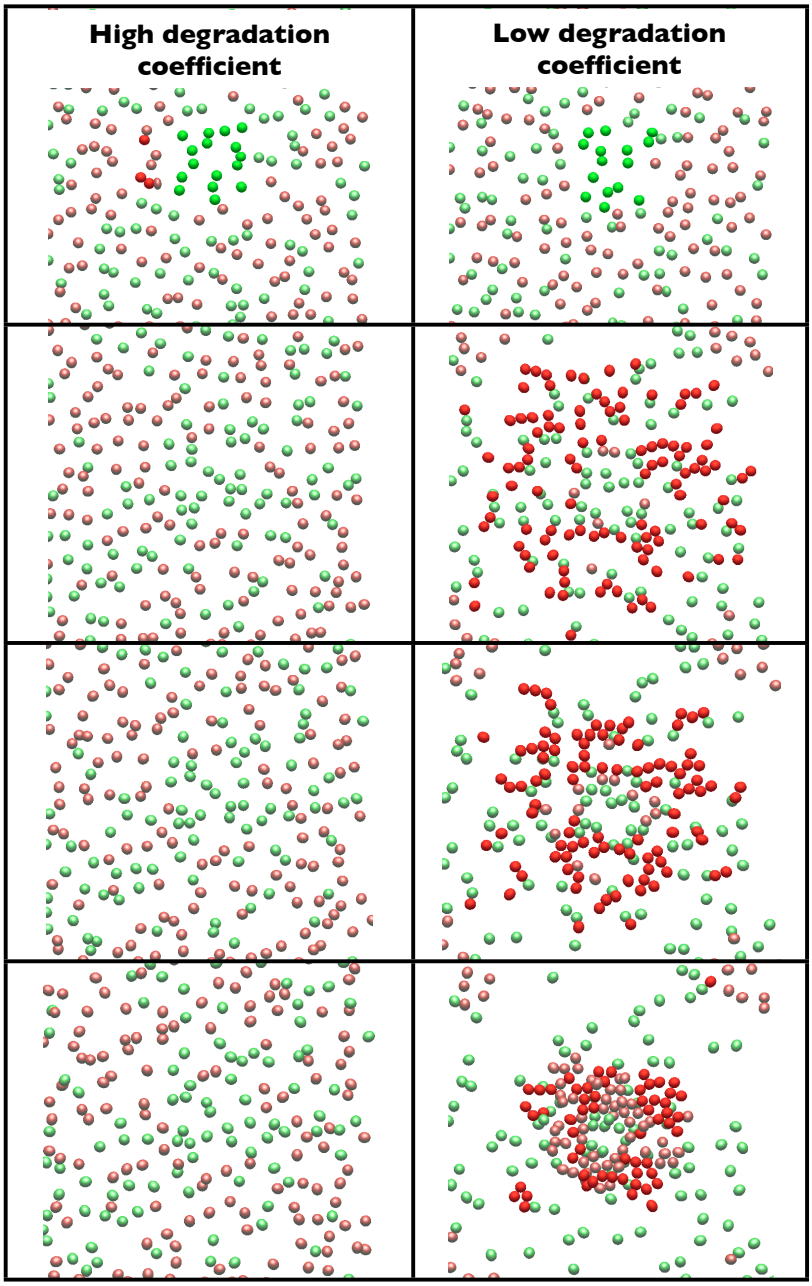

Figure A.6: Simulations conducted with the 3D model to compare to the results from the 1D system analysis. A perturbation in tumor cell (green cell) density is introduced in the centre. In the figures on the left side the degradation coefficients are high and the system stays at steady state. In the figures on the right side the degradation coefficients are low and the two cell types aggregate at the centre. The ratio between the two degradation coefficients stays constant.

Bibliography

[1] http://www.cancer.ca/. *Canadian cancer society*, 2012.

[2] J. Condeelis and J. W. Pollard. Macrophages: obligate partners for tumor cell migration, invasion, and metastasis. *Cell*, 124(2):263–6, Jan 2006.

[3] C. E. Lewis and J. W. Pollard. Distinct role of macrophages in different tumor microenvironments. *Cancer Res*, 66(2):605–12, Jan 2006.

[4] E. Y. Lin, A. V. Nguyen, R. G. Russell, and J. W. Pollard. Colony-stimulating factor 1 promotes progression of mammary tumors to malignancy. *Journal of experimental medicine*, 193(6):727–40, Mar 2001.

[5] E. Y. Lin, V. Gouon-Evans, A. V. Nguyen, and J. W. Pollard. The macrophage growth factor csf-1 in mammary gland development and tumor progression. *J Mammary Gland Biol Neoplasia*, 7(2):147–62, Apr 2002.

[6] J. B. Wyckoff, Y. Wang, E. Y. Lin, J.-f. Li, S. Goswami, E. R. Stanley, J. E. Segall, J. W. Pollard, and J. Condeelis. Direct visualization of macrophage-assisted tumor cell intravasation in mammary tumors. *Cancer Res*, 67(6):2649–56, Mar 2007.

[7] A. H. Beck, I. Espinosa, B. Edris, R. Li, K. Montgomery, S. Zhu, S. Varma, R. J. Marinelli, M. van de Rijn, and R. B. West. The Macrophage Colony-Stimulating Factor 1 Response Signature in Breast Carcinoma. *Clinical cancer research*, 15(3):778–787, Feb 1 2009.

[8] J. Pu, C. D. McCaig, L. Cao, Z. Zhao, J. E. Segall, and M. Zhao. EGF receptor signalling is essential for electric-field-directed migration of breast cancer cells. *Journal of cell science*, 120(19):3395–3403, Oct 1 2007.

[9] E. R. Andrechek and W. J. Muller. Tyrosine kinase signalling in breast cancer: tyrosine kinase-mediated signal transduction in transgenic mouse models of human breast cancer. *Breast Cancer Res*, 2(3):211–6, Apr 12 2000.

[10] E. T. Roussos, J. S. Condeelis, and A. Patsialou. Chemotaxis in cancer. *Nat Rev Cancer*, 11(8):573–87, Aug 2011.

[11] U. Philippar, E. T. Roussos, M. Oser, H. Yamaguchi, H.-D. Kim, S. Giampieri, Y. Wang, S. Goswami, J. B. Wyckoff, D. A. Lauffenburger, E. Sahai, J. S. Condeelis, and F. B. Gertler. A mena invasion isoform potentiates egf-induced carcinoma cell invasion and metastasis. *Dev Cell*, 15(6):813–28, Dec 2008.

[12] E. T. Roussos, Y. Wang, J. B. Wyckoff, R. S. Sellers, W. Wang, J. Li, J. W. Pollard, F. B. Gertler, and J. S. Condeelis. Mena deficiency delays tumor progression and decreases metastasis in polyoma middle-t transgenic mouse mammary tumors. *Breast Cancer Res*, 12(6):R101, 2010.

[13] C. T. Guy, R. D. Cardiff, and W. J. Muller. Induction of mammary tumors by expression of polyomavirus middle t oncogene: a transgenic mouse model for metastatic disease. *Mol Cell Biol*, 12(3):954–61, Mar 1992.

[14] K. M. Henkels, T. Farkaly, M. Mahankali, J. E. Segall, and J. Gomez-Cambronero. Cell invasion of highly metastatic mtln3 cancer cells is dependent on phospholipase d2 (pld2) and janus kinase 3 (jak3). *J Mol Biol*, 408(5):850–62, May 2011.

[15] W. Wang, S. Goswami, K. Lapidus, A. L. Wells, J. B. Wyckoff, E. Sahai, R. H. Singer, J. E. Segall, and J. S. Condeelis. Identification and testing of a gene expression signature of invasive carcinoma cells within primary mammary tumors. *Cancer Res*, 64(23):8585–94, Dec 2004.

[16] J. T. Price, T. Tiganis, A. Agarwal, D. Djakiew, and E. W. Thompson. Epidermal growth factor promotes mda-mb-231 breast cancer cell migration through a phosphatidylinositol 3'-kinase and phospholipase c-dependent mechanism. *Cancer Res*, 59(21):5475–8, Nov 1999.

[17] K. Knapek, K. Frondorf, J. Post, S. Short, D. Cox, and J. Gomez-Cambronero. The molecular basis of phospholipase d2-induced chemotaxis: elucidation of differential pathways in macrophages and fibroblasts. *Mol Cell Biol*, 30(18):4492–506, Sep 2010.

[18] D. Cox, P. Chang, Q. Zhang, P. G. Reddy, G. M. Bokoch, and S. Greenberg. Requirements for both rac1 and cdc42 in membrane ruffling and phagocytosis in leukocytes. *J Exp Med*, 186(9):1487–94, Nov 1997.

[19] C. Morgan, J. W. Pollard, and E. R. Stanley. Isolation and characterization of a cloned growth factor dependent macrophage cell line, bac1.2f5. *J Cell Physiol*, 130(3):420–7, Mar 1987.

[20] A. V. Vorotnikov. Chemotaxis: Movement, direction, control. *Biochemistry-moscow*, 76(13):1528–1555, Dec 2011.

[21] S. Goswami, E. Sahai, J. B. Wyckoff, M. Cammer, D. Cox, F. J. Pixley, E. R. Stanley, J. E. Segall, and J. S. Condeelis. Macrophages promote the invasion of breast carcinoma cells via a colony-stimulating factor-1/epidermal growth factor paracrine loop. *Cancer Res*, 65(12):5278–83, Jun 2005.

[22] J. Wyckoff, W. Wang, E. Y. Lin, Y. Wang, F. Pixley, E. R. Stanley, T. Graf, J. W. Pollard, J. Segall, and J. Condeelis. A paracrine loop between tumor cells and macrophages is required for tumor cell migration in mammary tumors. *Cancer Res*, 64(19):7022–9, Oct 2004.

[23] L. Soon, G. Mouneimne, J. Segall, J. Wyckoff, and J. Condeelis. Description and characterization of a chamber for viewing and quantifying cancer cell chemotaxis. *Cell Motil Cytoskeleton*, 62(1):27–34, Sep 2005.

[24] W. K. Raja, B. Gligorijevic, J. Wyckoff, J. S. Condeelis, and J. Castracane. A new chemotaxis device for cell migration studies. *Integr Biol (Camb)*, 2(11-12):696–706, Nov 2010.

[25] N. Kirma, R. Luthra, J. Jones, Y.-G. Liu, H. B. Nair, U. Mandava, and R. R. Tekmal. Overexpression of the colony-stimulating factor (csf-1) and/or its receptor c-fms in mammary glands of transgenic mice results in hyperplasia and tumor formation. *Cancer Research*, 64(12):4162–4170, 2004.

[26] E. Palsson. A 3-d model used to explore how cell adhesion and stiffness affect cell sorting and movement in multicellular systems. *J Theor Biol*, 254(1):1–13, Sep 2008.

[27] R. G. Thorne, S. Hrabětová, and C. Nicholson. Diffusion of epidermal growth factor in rat brain extracellular space measured by integrative optical imaging. *Journal of Neurophysiology*, 92(6):3471–3481, 2004.

[28] D. Bray. *Cell movements*. Garland Publishing Inc, 1992.

[29] S. Giampieri, C. Manning, S. Hooper, L. Jones, C. S. Hill, and E. Sahai. Localized and reversible TGF beta signalling switches breast cancer cells from cohesive to single cell motility. *Nature cell biology*, 11(11):1287–U49, Nov 2009.

[30] A. Patsialou, J. Wyckoff, Y. Wang, S. Goswami, E. R. Stanley, and J. S. Condeelis. Invasion of human breast cancer cells in vivo requires both paracrine and autocrine loops involving the colony-stimulating factor-1 receptor. *Cancer Res*, 69(24):9498–506, Dec 2009.

[31] D. B. Hoelzinger, T. Demuth, and M. E. Berens. Autocrine factors that sustain glioma invasion and paracrine biology in the brain microenvironment. *J Natl Cancer Inst*, 99(21):1583–93, Nov 2007.

[32] M. Luca, A. Chavez-Ross, L. Edelstein-Keshet, and A. Mogilner. Chemotactic signaling, microglia, and alzheimer's disease senile plaques: Is there a connection? *Bulletin of mathematical biology*, 65(4):693–730, Jul 2003.